2022

Viral overexpression of RPRD2 in mouse nucleus accumbens induces anxiety-like behavior and regulates genes associated with microtubule transport

Claire Nuhad Atiyeh

Viral overexpression of RPRD2 in mouse nucleus accumbens induces anxiety-like behavior and regulates genes associated with microtubule transport

A thesis submitted in partial fulfillment of the requirements for the degree of Master of Science in Anatomy and Neurobiology at Virginia Commonwealth University.

By
Claire N. Atiyeh
B.S. Kinesiology and Health Sciences, William & Mary, 2020

Advisor: Peter J. Hamilton, Ph.D.
Assistant Professor
Department of Anatomy and Neurobiology

Virginia Commonwealth University
Richmond, VA

April 2022
Acknowledgements

I would like to acknowledge all members of the Hamilton Lab for their support and assistance in this endeavor. I would like to thank Joey Picone and Gabby Silva for their aid in performing surgeries, Kijoon Kim for his assistance in bioinformatics and perfusions, and Natalie Truby for her direction when performing medium spiny neuron morphologies. To Xiaohong Cui, thank you for the countless hours spent training me to conduct Western blots. To Hannah Woolard, thank you for your utmost guidance and partnership throughout this project. Most importantly, thank you Dr. Peter Hamilton for the mentorship and patience you have given me, and for creating such a supportive and knowledgeable team within the lab. Additional thanks to my family for all their moral support throughout these past years.

Table of Contents

Page

List of Figures

List of Abbreviations

Abbreviation……………..Explanation

NAc…………………………..Nucleus Accumbens

RPRD2………………………Regulation of Nuclear Pre-mRNA Domain Containing 2

REAF………………………...RNA-associated Early-stage Antiviral Factor

COVID-19………………….CoronaVirus Disease 2019

S5p…………………………..Phosphorylation of Serines at Position 5

GFP…………………………..Green Fluorescent Protein

HSV………………………….Herpes Simplex Virus

PBS…………………………..Phosphate Buffered Saline

CSDS………………………..Chronic Social Defeat Stress

SI……………………………..Social Interaction

EPM…………………………Elevated Plus Maze

TBST…………………………Tris Buffered Saline with Tween 20

BSA…………………………..Bovine Serum Albumin

GO……………………………Gene Ontology

PFA…………………………..Paraformaldehyde

MSN…………………………Medium Spiny Neuron

ANOVA   ……………………..Analysis of Variance

DEG…………………………Differentially Expressed Gene

AAV…………………………..Adeno-associated Virus

Abstract

VIRAL OVEREXPRESSION OF RPRD2 IN MOUSE NUCLEUS ACCUMBENS INDUCES ANXIETY-LIKE BEHAVIOR AND REGULATES GENES ASSOCIATED WITH MICROTUBULE TRANSPORT

Claire N. Atiyeh

A thesis in partial fulfillment of the requirements for the degree of Master of Science in Anatomy and Neurobiology at Virginia Commonwealth University.

Virginia Commonwealth University, 2022

Peter J. Hamilton, Ph.D., Assistant Professor, Department of Anatomy and Neurobiology

Anxiety disorders are the most prevalent mental illness in the United States with many individuals underdiagnosed and undertreated (Anxiety & Depression Association of America, 2021; Bandelow et al., 2017). While stress is a known risk factor for developing anxiety disorders, there is emerging evidence that biological variability in the expression of key proteins in the brain may contribute to regulating an organism's stress-related behaviors. Earlier work from our laboratory identified a protein, called Regulation of Nuclear Pre-mRNA Domain Containing 2 (RPRD2), that was differentially expressed in the brain of mice stratified in terms of their phenotypic response to chronic stress (Hamilton et al., 2020). RPRD2 protein was elevated in the nucleus accumbens (NAc) of stress resilient animals–mice that display fewer behavioral abnormalities and more successful adaptation to stressors–and is predicted to play a significant role in gene transcription (Hamilton et al., 2020; Sjöstedt et al., 2020). In a cohort of mice exposed to chronic social defeat stress (CSDS), this protein was revealed as differentially expressed in the ventral hippocampus, medial prefrontal cortex, and NAc, of which RPRD2 was the top most affected protein in the NAc (Hamilton et al., 2020). More specifically, previously

published reports suggest that RPRD2 functions to modulate RNA polymerase II activity by dephosphorylating serines at position 5 of the carboxyl-terminal domain of RNA polymerase II (Sjöstedt et al., 2020). Due to the correlation between RPRD2 and stress-induced behavioral adaptations in laboratory rodents, I aim to build upon this data and decipher this protein's influence on stress-related behavior, mechanism of action in the NAc, and any potential impact it may have on medium spiny neuron (MSN) morphology, the major neuron functional unit in the NAc.

In order to expand upon the work conducted by Hamilton et al., I first exposed mice to a period of CSDS and conducted behavioral tests to determine the extent to which elevated levels of RPRD2 in the NAc impacted behavior. Following a period of CSDS, male mice with viral overexpression of RPRD2 spent less time in the open arms of an Elevated Plus Maze (EPM) test, a paradigm that quantifies anxiety-like behavior; however, no difference was observed with a Social Interaction test or thigmotaxis analysis–the tendency of mice to remain close to the walls (Bailey & Crawley, 2009; Kraeuter et al., 2019; Rodgers & Dalvi, 1987). These findings support the conclusion that viral overexpression of RPRD2 specifically impacts anxiety-like behavior, rather than social behavior–another behavioral domain known to be sensitive to chronic stress.

I then began to inquire about not only RPRD2's behavioral impact, but also RPRD2's molecular impact in the NAc. It was previously reported that RPRD proteins recruit deacetylases of lysine residues at position 7–specifically, HDAC1–which in turn allows RPRD to decrease phosphorylation of serines at position 5 of the carboxyl-terminus domain of RNA Polymerase II (Ali et al., 2019). Because RNA polymerase II facilitates transcription, I examined RPRD2's impact on its Phospho Serine 5 levels via Western blots in order to explore its particular role in

transcription. Although no significant correlation was found, tissue samples from mice virally overexpressed with RPRD2 revealed a downward trend in RNA Polymerase II Phospho Serine 5 levels (normalized to β-actin). This led me to further inquire about the exact downstream mechanistic impact of this protein and its regulation of transcription within the NAc.

We performed RNA sequencing to determine the gene loci regulated by viral over-expression of RPRD2 in the NAc. RPRD2 overexpression was correlated with upregulated genes canonically enriched in fibroblast cell-types and associated with downregulated genes enriched in ependymal cell-types. Following a gene ontology analysis performed on the significantly regulated differentially expressed genes (DEGs) in the RNA sequencing data, microtubule-based movement was the biological process most significantly associated with RPRD2 downregulated transcripts. Due to this finding, more research is needed regarding the impact of viral overexpression of RPRD2 on downregulating microtubule transport within RPRD2 expressing cells in the NAc.

Furthermore, previous studies have shown decreased strength of NAc synapses of mice expressing depression-like behavior following CSDS (Bagot et al., 2015; LeGates et al., 2018). Thus, enhancing activity in MSNs may result in resilient behavior; contrastingly, diminishing MSNs may result in anxiety-like behavior following CSDS (Francis & Lobo, 2017). To test this, I observed the contribution of viral overexpression of RPRD2 on medium spiny neuron morphology. Based on observation, there appeared to be less dendritic branching in neurons virally overexpressed with RPRD2; however, a Sholl analysis must be conducted in the future in order to solidify this observation.

Overall, I hypothesize that viral overexpression of RPRD2 in the NAc regulates anxiety-like behavior by decreasing RNA polymerase II-mediated transcriptional activity, which consequently impacts medium spiny neuron morphology in the NAc. In synthesizing my research, I will describe my comprehensive knowledge of RPRD2 and its relationship to chronic stress and anxiety, as well as a description of the materials and methods used to demonstrate the effects of RPRD2 in the NAc. I will then describe the results collected and discuss its potential ramifications in understanding the molecular drivers of neuropsychiatric syndromes. The results of this study can help to better understand how RPRD2 serves as a link between chronic stress and behavioral responses, and the mechanistic role of RPRD2 in the NAc. In the future, I hope this data can facilitate studies dedicated to targeting RPRD2 in order to develop effective pharmacotherapies for those with anxiety disorders.

Introduction

Anxiety disorders are the most prevalent mental illness in the United States, affecting 18.1% of the population–ages 18 or older–each year (Anxiety & Depression Association of America, 2021). Despite their prevalence, anxiety disorders often go underrecognized and undertreated, with only 36.9% of those suffering receiving treatment (Anxiety & Depression Association of America, 2021; Bandelow et al., 2017). Below, I review data related to the contributions of RPRD2 on anxiety-like behavior. Regulation of nuclear pre-mRNA domain containing 2 (RPRD2) is an understudied protein that is implicated in regulating RNA polymerase II binding activity and mRNA 3' end processing (Alliance of Genome Resources, 2021). Emerging evidence suggests that resilient mice–or mice that display fewer stress-induced behavioral abnormalities and more successful behavioral adaptation to stressors–have higher levels of RPRD2 protein within the NAc in comparison to susceptible mice–or mice that develop stress-induced behavioral deficits– when exposed to chronic social defeat stress (Hamilton et al., 2020; Wendelmuth et al., 2020). To explore this further, I hypothesized that mice with viral overexpression of RPRD2 in the NAc would display fewer anxiety-like behaviors when exposed to chronic stress than mice without.

Evidence also suggests that RPRD proteins decrease phosphorylation of serines at position 5 on the carboxyl-terminus domain of RNA polymerase II (Ali et al., 2019). Thus, I hypothesized that mice with viral overexpression of RPRD2 would show less phosphorylation of serines at position 5 and therefore lower levels of transcription due to reduced RNA polymerase II activity. Additionally, previous studies have shown decreased strength of NAc

synapses of mice expressing depression-like behavior following CSDS (Bagot et al., 2015; LeGates et al., 2018). Due to this evidence, enhancing activity in MSNs may result in resilient behavior while diminishing MSNs may result in depression-like behavior following CSDS (Francis & Lobo, 2017). Should these mice not show resilience, I hypothesized that there would be a decrease in MSN dendrites following viral overexpression of RPRD2. Collectively, an understanding of RPRD2 and its impact on brain and behavior will build a stronger framework behind the mechanism of anxiety disorders. In addition, these data will raise awareness regarding the implications of chronic stress within the NAc.

CoronaVirus Disease 2019

Fear of the unknown leads to higher anxiety levels in both those with and without pre-existing mental health conditions (Torales et al., 2020). Currently, very little is known about the CoronaVirus Disease 2019 (COVID-19); therefore, it poses a global risk to mental health (Talevi et al., 2020). COVID-19 is a pandemic caused by the novel Coronavirus strain SARS-CoV-2 (Talevi et al., 2020). Quarantine, isolation, and social distancing has been enacted in order to restrict COVID-19 transmission. The World Health Organization warns that these restrictions and disruptions in people's routines may lead to loneliness, anxiety, depression, insomnia, harmful alcohol/drug use, and suicidal behavior (Selçuk et al., 2021). This statement is further solidified by a study conducted in the United Kingdom in which, of the 44% suffering cluster of people, 93% report feeling more anxious and depressed since lockdown measures were introduced (Duffy et al., 2020).

Psychological reactions to pandemics include maladaptive behaviors, emotional distress, and defensive responses such as: anxiety, fear, frustration, loneliness, anger, boredom, depression, stress, and avoidance behaviors (Talevi et al., 2020). In particular, headline stress disorder can be observed in which further progression to physical and mental disorders may be observed due to a high emotional response–such as stress and anxiety–to reports from the news media (Talevi et al., 2020). COVID-19 related chronic stress has profound impacts on long-term mental health (Qi et al., 2021). Findings from China suggest that more than 25% of the general population experienced moderate to severe levels of stress and/or anxiety-related symptoms in response to COVID-19 (Nikčević & Spada, 2020). Even one year after the first COVID-19 outbreak, the prevalence of anxiety in the general population has not changed (Qi et al., 2021). This indicates that the impact of the pandemic on mental health has not been attenuated despite control of its spread. COVID-19 impact on mental health may be long-lasting. Hopefully, the data presented below may aid in understanding the mechanism behind and in developing effective pharmacotherapies for the large portion of the population suffering from anxiety disorder.

Chronic Stress and Anxiety

Stress can be both objective and subjective with respect to physical and psychological stressors (Mariotti, 2015). Unpleasant, aversive, or threatening situations initiate a stress response in the body in order to allow it to properly cope with the stress (Lucassen et al., 2014). In humans, unpleasant surprises, injuries, financial difficulties, loss, physical threats, etc. are all

examples of different types of stressors. Stress becomes chronic during instances in which the stressor becomes overwhelming and unresolvable over a period of time (Mariotti, 2015). Physiologically, glucocorticoid receptors in the brain that normally provide a negative feedback mechanism to regulate the stress response become resistant, and systemic levels of stress-related molecular mediators remain high (Mariotti, 2015). This in turn damages multiple organs and tissues long term (Mariotti, 2015). Diseases linked to stress include cardiovascular dysfunctions, diabetes, cancer, autoimmune syndromes, and mental illnesses such as depression and anxiety disorders (Lucassen et al., 2014; Mariotti, 2015).

Stress is the most common risk factor for the development of depression and anxiety disorders (Lucassen et al., 2014; Pêgo et al., 2010). About one-half of those with depression disorder are also diagnosed with an anxiety disorder, and the two are often considered comorbid disorders (Anxiety & Depression Association of America, 2021). These two comorbid disorders suggest the existence of an anxiety–depression spectrum according to measures of distress and fear (Hoffman, 2015). Two examples on the "distressed end" of this spectrum are generalized anxiety disorder and major depressive disorder. Generalized anxiety disorder is the most common anxiety disorder affecting 3.1% of the United States population, while major depressive disorder affects 6.7% of the United States population (Anxiety & Depression Association of America, 2021). Examples on the "fear end" of this spectrum are panic disorder, affecting 2.7% of U.S. adults, and specific phobias, affecting 8.7% of U.S. adults. Social anxiety disorder is another example of an anxiety disorder, and obsessive-compulsive disorder and post-traumatic stress disorder are closely related. Treatment for these disorders include:

psychotherapy, pharmacotherapy, exercise, support groups, stress management techniques, hypnosis, and complementary medicine methods (Bandelow et al., 2017).

Nucleus Accumbens

The nucleus accumbens (NAc) is connected to the limbic system of the brain and is the most inferior part of the striatum, which comprises the caudate nucleus and the putamen (Mavridis, 2015). As part of the reward circuitry in the brain, the NAc plays a key role in food intake, sexual behavior, reward-motivated behavior, stress-related behavior and substance-dependence stress-related behavior (Mavridis, 2015; Sjöstedt et al., 2020). Evidence has shown that deep brain stimulation of the NAc is correlated with antidepressant and anxiolytic effects (Mavridis, 2015). As such, changes in the NAc affect psychiatric disorders such as depression, schizophrenia, substance abuse disorder, obsessive-compulsive disorder, and anxiety disorders.

The nucleus accumbens receives dopaminergic inputs from the ventral tegmental area (Baik, 2020). Dopamine is produced in the substantia nigra and ventral tegmental area of the midbrain and is involved with reward, mood, pleasure, smooth motor movements, focus, and attention. Shortages in dopamine lead to aggression, compulsive behavior, overeating, and depression. (Sheffler, 2021). The NAc also receives glutamatergic inputs from the hippocampus, prefrontal cortex, basolateral amygdala, and thalamus (Baik, 2020; Bagot et al., 2015). Glutamate is the primary excitatory neurotransmitter in the brain and glutamate deficiency leads to fatigue, lack of focus, apathy (Bagot et al., 2015). Medium spiny neurons (MSNs) are the primary neurons that integrate these cortico-limbic afferens with the NAc as the afferents

terminate on the MSN dendritic spines, which are capable of storing information and

transmitting electrical signals (Dobrof & Penrod-Martin, 2012; Lucassen et al., 2014).

MSNs from the NAc also project GABA/gamma aminobutyric acid outputs to the ventral

pallidum, the medial area of the globus pallidus, the substantia nigra, and the lateral

hypothalamus (Baik, 2020; Dobrof & Penrod-Martin, 2012). GABA is the primary inhibitory

neurotransmitter in the brain and shortages lead to stress and anxiety, depression, ADHD, panic

disorders, and many others (Sheffler, 2021). For example, animals displaying anhedonia and

depression-like behavior reveal an enlargement of MSNs in the NAc (Bessa et al., 2013).

NAc and Stress

Stress affects the dopamine levels in the brain (Baik, 2020). Long-term, chronic stress

weakens reward sensitivity by dampening the ability to cope with stressors and recruit

appropriate reward-related neural connections (Baik, 2020). Stressful events negatively

regulate dopaminergic neuronal activity which can lead to chronic stress-induced depression

(Baik, 2020). Stress can also cause reduction in volume of structures within the brain and

changes in neuronal plasticity due to decreased spine density (Lucassen et al., 2014).

Chronic social defeat stress (CSDS) is a widely utilized laboratory technique to induce

depression-like and anxiety-like behaviors in rodents, as is demonstrated by anhedonia and

social avoidance (Golden et al., 2011). Glutamatergic afferents to the NAc regulate

susceptibility and resiliency to CSDS in rodents (Bagot et al., 2015). Previous studies have shown

a decrease in both the glutamatergic transmission of prefrontal cortex-NAc synapses and the

strength of hippocampus-NAc synapses of mice expressing depression-like behavior following

CSDS (Bagot et al., 2015; LeGates et al., 2018). Thus, diminishing MSN function may result in

susceptible, depression-like behavior following CSDS (Francis & Lobo, 2017).

Rodent models are leading neuropsychiatric research as they can aid in the assessment

of endophenotypes for anxiety disorders (Bailey & Crawley, 2009; Hoffman, 2015).

Manipulation of the protein expression in the brain, application of stressors, and quantification

of different behavioral paradigms were all used in order to model stress and assess anxiety-like

behavior.

Regulation of Nuclear Pre-mRNA Domain Containing 2

Emerging evidence suggests that resilient mice have higher levels of RPRD2 within the

NAc in comparison to susceptible mice when exposed to chronic social defeat stress (Hamilton

et al., 2020; Wendelmuth et al., 2020). In fact, RPRD2 was the only protein affected across the

three brain areas investigated in this study: the ventral hippocampus, the medial prefrontal

cortex, and the NAc (Hamilton et al., 2020). It was also the top most affected protein in the NAc

of a cohort of mice exposed to CSDS (Hamilton et al., 2020). Given the bi-directional regulation

of RPRD2 in resilient versus susceptible animals in multiple limbic brain regions and its

magnitude of effect in the NAc, we felt this data warranted additional inquiry about the role of

this understudied protein on stress-exposed mice.

RPRD2–also referred to as REAF (RNA-associated early-stage antiviral factor) in certain

literature–is elevated in the NAc of resilient animals and is predicted to play a significant role in

gene transcription (Hamilton et al., 2020; Sjöstedt et al., 2020). RPRD2 is a protein that binds to

the carboxyl-terminal domain (CTD) of RNA polymerase II and restricts its function (Sjöstedt et al., 2020). It is predicted to be involved in mRNA 3'-end processing (Alliance of Genome Resources, 2021). Thus, higher levels of RPRD2 may lead to less mRNA transcribed from DNA; yet, the gene loci most sensitive to this regulation remain unknown.

Other regulation of nuclear pre-mRNA domain homologs also exist: RPRD1A and RPRD1B. The two share similar amino acid sequences and domains (Ni et al., 2011). All three RPRD proteins contain CTD-interaction domains, and are expressed in the majority of human cell types and tissues. RPRD2 is much larger, with a length of around 1460 amino acids, a mass of 150,000 Daltons, and serine and proline rich regions (Ni et al., 2011; Sjöstedt et al., 2020).

RPRD2 and RNA Polymerase II

The CTD of RNA polymerase II contains repeats of the sequence Y1-S2-P3-T4-S5-P6-S7 (Ni et al., 2014). The total amount of CTD repeats varies in different organisms; however, homo sapiens and mus musculus both contain 52 heptad repeats on the CTD (Srivastava & Ahn, 2015). 21 of the heptad repeats are in consensus, while 31 diverge from the consensus (Ali et al., 2019). This divergence occurs most commonly at position 7, in which S7 can be replaced with N7 (arginine), T7 (threonine), or K7 (lysine) (Ali et al., 2019; Srivastava & Ahn, 2015). Lysine residues at position 7 are needed for transcription elongation (Ali et al., 2019). Acetylation of lysine residues at position 7 occurs at around 80% of actively transcribed genes, which indicates its role in regulating the transition from transcription initiation to elongation.

During early transcription, a mediator complex is recruited to the gene promoter of unphosphorylated RNA polymerase II (Srivastava & Ahn, 2015). This mediator complex then stimulates cyclin-dependent kinase 7–a subunit of the general transcription factor TFIIH–in mammals to phosphorylate S5 and S7 on the CTD of RNA polymerase II. Specifically, S5p aids in the transition from transcription initiation to elongation by inducing the dissociation of the mediator from the pre-initiation complex, stimulating RNA polymerase II for promoter clearance, and recruiting pre-mRNA capping enzymes (Ali et al., 2019; Srivastava & Ahn, 2015). Thus, dephosphorylation of S5p may cause a stall in the transition from transcription initiation to elongation.

Different mechanisms can be used to create a CTD code that acts as a scaffold and recruits regulators of transcription which post-translationally modify RNA polymerase II (Ali et al., 2019; Ni et al., 2014). Specifically, RPRD proteins have been found to control the CTD phosphorylation activity by reducing CTD S5- and S7-phosphorylated RNA polymerase II (Ni et al., 2011).

Evidence has shown that acetylation of lysine residues at position 7 regulates the phosphorylation of serines at position 5 (S5p) (Ali et al., 2019). First, acetylation of lysine residues at position 7 enhances binding to the CTD-interacting domain of RPRD proteins and recruits RPRD proteins to the initiated RNA polymerase II complex. S2p also enhances the interaction between the RNA polymerase II CTD and RPRD CTD-interaction domains (Ni et al., 2014). Then, RPRD proteins recruit deacetylases of lysine residues at position 7–specifically, HDAC1–which in turn allows RPRD to decrease phosphorylation of S5p (Ali et al., 2019).

Researchers posit that RPRD proteins facilitate S5p dephosphorylation by RNA polymerase II associated protein 2, their interacting S5 phosphatase (Ali et al., 2019; Srivastava & Ahn, 2015).

As mentioned, evidence suggests that resilient mice have higher levels of RPRD2 within the NAc in comparison to susceptible mice when exposed to chronic social defeat stress (Hamilton et al., 2020; Wendelmuth et al., 2020). As stress is the most common risk factor for the development of depression and anxiety disorders, and the two are often considered comorbid disorders, viral overexpression of RPRD2 in the NAc may regulate anxiety-like behaviors (Anxiety & Depression Association of America, 2021; Lucassen et al., 2014; Pêgo et al., 2010). This regulation may occur mechanistically through RPRD2's potential impact on gene transcription as evidenced by RPRD proteins and their dephosphorylation of S5p on the CTD of RNA polymerase II (Ali et al., 2019; Ni et al., 2014). Additionally, previous studies have shown a decrease in both the glutamatergic transmission of prefrontal cortex-NAc synapses and the strength of hippocampus-NAc synapses of mice expressing depression-like behavior following CSDS (Bagot et al., 2015; LeGates et al., 2018). Due to this evidence, enhancing activity in MSNs may result in resilient behavior while diminishing MSNs may result in anxiety-like behavior following CSDS (Francis & Lobo, 2017). A decrease in MSN dendrites following viral overexpression of RPRD2 may be observed should these mice not show resilience.

I hypothesized that mice with increased levels of RPRD2 in the NAc will display less anxiety-like behavior, will yield decreased phosphorylation of S5p on RNA polymerase II, and will demonstrate increased medium spiny neuron morphology following a period of chronic social defeat stress. Furthermore, utilized RNA sequencing approaches identified the gene loci most sensitive to RPRD2-mediated inhibition of RNA polymerase II function. In discerning the

transcriptional impact of RPRD2 overexpression with the RNA sequencing data, RPRD2 may be

targeted in order to develop effective pharmacotherapies for those with anxiety disorders.

Following a description of the materials and methods utilized in this study, I will outline the

data collected and discuss the implications of the results in this study.

Materials and Methods

Animal Husbandry

Adult male 8–10-week-old C57BL/6J mice and male 4–6-month-old CD1 retired breeder aggressor mice from Jackson Laboratories were housed at 22-25 °C in a 12-hour light/dark cycle. The animals were provided food and water as needed. C57BL/6J mice were paired in groups of five same-condition (HSV-RPRD2 or HSV-GFP) static cages for the duration of the study (Bailey & Crawley, 2009). CD1 mice were housed individually in static cages. All studies were conducted in accordance with the Institutional Animal Care and Use Committee regulations at Virginia Commonwealth University School of Medicine.

Stereotaxic Surgery

RPRD2 had been successfully gateway cloned in p1005 plasmid and packaged in Herpes Simplex Virus (HSV) by Hannah Woolard, another Master's student in the Hamilton Lab, for further use. Stereotaxic surgery was conducted in order to virally inject HSV-RPRD2 or HSV-GFP into the NAc of mice. Mice were anesthetized with a Ketamine/Xylazine mixture (100 mg/kg Ketamine and 5 mg/kg Xylazine dissolved in sterile normal saline) injected into the peritoneum. The eyes were covered with an ocular lubricant to prevent dryness during the surgery. Mice were securely placed on clean stereotaxic instruments with the skull surface exposed; the instruments were routinely sterilized with 70% acetone, and the syringes (5 μL Microliter Syringe Model 85 RN, Small Removable Needle, 26s gauge, 2 in, point style 2) were sterilized

with 100% acetone and PBS. Betadine antiseptic was applied to the top of the head using sterile cotton swabs and a middle incision was made with a disposable razor. The tip of the syringes were positioned at Bregma, an anatomical landmark on the rodent's skull. The x, y, and z coordinates were zeroed out on a digital Vernier scale to set Bregma as an origin point in respect to all other coordinates. To locate the NAc, the syringes were positioned to pre-calculated anterior/posterior and medial/lateral coordinates at +1.6 and -1.5/+1.5 respectively (Franklin & Paxinos, 2019). The area of the skull directly under the syringe tips was drilled using a dental drill with a 0.6 mm burr. 1 µL of the virus (viral aliquots stored in a -80 °C freezer, transported on dry ice, and kept on wet ice when in use) was acquired and the syringes were lowered to the dorsal/ventral coordinate at -4.4. The viral solution was delivered at a rate of 0.2 µL per minute and syringes were held for five minutes following delivery to allow the virus to diffuse. The syringes were slowly raised out of the skull and the animal was removed from the stereotaxic instrument. The incision was closed via tissue adhesive. Animals were placed in a clean cage warmed on an IR heating pad during recovery from the anesthesia. The heating pad was removed and the mice given one day to acclimate before experiencing chronic social defeat stress. This process was conducted with the aid of Joey Picone, Natalie Truby, Gabriella Silva, and Kijoon Kim: graduate students in the Hamilton lab who were trained on this procedure.

Chronic Social Defeat Stress

A Chronic Social Defeat Stress (CSDS) protocol was implemented to establish anxiety-like behavior in cohorts of 20 mice (Golden et al., 2011). Although a standard CSDS protocol from

previous studies occurs for 10 minutes, twice a day, for 10 days, an accelerated CSDS protocol

was chosen for this experiment as HSV target and expression in neurons is only evident for 3-7

days. As a control to negate stress as a factor, the first cohort did not experience CSDS. The

second cohort of mice experienced CSDS for 10 minutes, twice a day, for 5 days. The third and

fourth cohort experienced a more aggressive CSDS for 11 minutes, twice a day, for 6 days in

order to further power the results and more closely mimic the standard CSDS protocol. The fifth

cohort also did not experience CSDS **(Figure 1)**. C57BL/6J mice were individually housed in static

cages with a perforated divider. To experience physical stress, the C57BL/6J mice were exposed

to a novel CD1 aggressor mouse on the same side of the perforated divider for an allotted

duration. Following CSDS, the C57BL/6J mice were transferred to the other side of the

perforated divider to stimulate sensory stress from the neighboring CD1 mouse. The C57BL/6J

mice encountered a novel CD1 mouse for each defeat. This process was conducted both by

myself and with the aid of Hannah Woolard.

Behavioral Testing

Behavioral testing was conducted 24 hours after the final CSDS. Behavioral testing

consisted of a social interaction test and an elevated plus maze test. From the social interaction

test, heat maps and thigmotaxis data were acquired. Behavioral testing was conducted under a

red light, and video recorded and tracked using Ethovision XT. The first cohort (No CSDS)

consisted of nine HSV-GFP mice and eight HSV-RPRD2 mice, the second cohort (5 Day CSDS)

consisted of nine HSV-GFP mice and nine HSV-RPRD2 mice, the third cohort (6 Day CSDS)

consisted of seven HSV-GFP mice and seven HSV-RPRD2 mice, the fourth cohort (6 Day CSDS) consisted of two HSV-GFP mice and three HSV-RPRD2 mice, and the fifth cohort (No CSDS) consisted of two HSV-GFP mice and two HSV-RPRD2 mice. The following processes were conducted both by myself and with the aid of Hannah Woolard.

Social Interaction Test

A social interaction (SI) test was conducted to measure social behavior (File & Hyde, 1978). First, a C57BL/6J mouse was allowed to freely explore a 53 x 53 cm arena with walls 43 cm high containing an empty plexiglass wire mesh cage against one wall of the arena for 2.5 minutes. The mouse was removed and the arena cleaned with 70% ethanol. Then, a novel CD1 aggressor mouse was placed in the plexiglass wire mesh cage. The same C57BL/6J mouse was placed in the center of the arena for 2.5 minutes to test time spent in the interaction zone (18 x 25 cm) during sensory exposure to the aggressor mouse. The same CD1 aggressor mouse was used for each arena to provide consistent social interaction.

Elevated Plus Maze Test

Immediately after the SI test, an elevated plus maze (EPM) test was conducted to further measure anxiety-like behavior (Bailey & Crawley, 2009; Kraeuter et al., 2019; Rodgers & Dalvi, 1987). The EPM arena was elevated off of the floor (63.5 cm high) and consisted of two opposite open arms crossed by two opposite closed arms with a center area at the crossing. A

C57BL/6J mouse was placed in the center area and allowed to explore the arena for five minutes to assess time spent in the open arms (each arm was 38 cm long). The mouse was removed and the arena cleaned with 70% ethanol.

Thigmotaxis

Thigmotaxis was measured using the SI test data to determine the tendency of mice to remain close to the walls, indicating increased fear or anxiety with decreased time spent in the center zone (17 x 32 cm) (Simon et al., 1994).

Tissue Collection

Following rapid decapitation, brains were removed and sectioned into 1 mm coronal slices using brain matrices. Using two 14-gauge punches under a fluorescent light, bilateral NAc tissue samples were extracted, placed into individual Eppendorf tubes (1.5 mL), frozen on dry ice, and stored in a -80 °C refrigerator until Western Blots were conducted. Tissue collection was conducted with the aid of Joey Picone, Natalie Truby, Gabriella Silva, and Kijoon Kim.

Western Blot

Western Blots were conducted to measure levels of protein in the tissue samples collected. 200 μL of ice-cold RIPA buffer was added to the sample in the 1.5 mL Eppendorf tube

(Bio-Rad Laboratories, Inc., n.d.). Samples were homogenized with battery-operated mortar and pestle with sterile blue tips until no tissue pieces were apparent and sonicated for 3 cycles of 20 seconds on wet ice in a cold room (BioRuptor: 120w). The probe was rinsed with 70% ethanol and dried with Kim wipes between each sample. The tubes were shaken on Effendorf ThermoMixer at 4°C and 300 rpm for 30 minutes, and then centrifuges at 14,000 rpm at 4 °C for 15 minutes. 170 μL of the supernatant was transferred to a new 1.5 mL Eppendorf tube and the rest was saved in the -80 °C refrigerator. Total protein levels were determined using a proprietary colorimetric detection reagent (Pierce660 nm Protein Assay Kit). Sample concentrations were normalized with RIPA buffer, mixed with equal amounts of 2x Laemmli buffer, and pipetted up and down 20 times to mix. 60 μL of the sample was aliquot in a 1.5 ml Eppendorf tube. Under a hood, 5 μL of bME was added to the sample and mixed 10 times. The sample was heated at 95 °C for 5 minutes and then vortexed (medium speed, 2000 rpm, 30 seconds). TGX stain free gel (BIO-RAD; catalog number 5678094) were assembled and the tank filled with a 10:1 ratio of deionized water and 10x Tris/Glycine/SDS buffer. 15 μL of each sample and 10 μL of the well standards (Precision Plus Protein Unstained Standards and Precision Plus Protein Kaleidoscope) were loaded into the gel which was run at 100 V for 2 hours. The gel was transferred onto a membrane using the Transblot Turbo Packs (BIO-RAD; catalog number 1704157, high molecular weight, 2.5A constant, up to 25 V, 10 minutes). A stain-free gel image was obtained using the ChemiDoc MP Imaging System. The membrane was placed in 50 mL of blocking buffer (7% milk/TBST) and rocked on a rocking platform at room temperature for 1 hour. The buffer was removed and the membrane washed twice with TBST. The primary antibody was placed to cover the membrane and rock overnight at room temperature [Goat

pAb to RPRD2 50 ug (1 mg/mL), Ab10363, Primary Ab 1:2000/2.5% BSA, 17 µL and 35 mL]. The following day, the membrane was washed with TBST and rocked in TBST for 10 minutes at room temperature three times. 5 µL of the secondary antibody [Dnk pAb to Goat IgG (HRP) 500 ug (2 mg/mL), Ab205723, Secondary Ab 1:10000] was diluted in 50 mL of 2.5% milk and rocked at room temperature for 1 hour. The membrane was washed five times with TBST for 10 minutes. The membrane was placed in 10 mL of Clarity ECL substrate kit components (BIO-RAD; catalog number 170-5060), and a chemiluminescent and calorimetric image was obtained using the ChemiDoc MP Imaging System. The membrane was rinsed in TBST and unblocked with 5% milk at room temperature for 1 hour. The membrane was rinsed again with TBST twice before another primary antibody was added and the method repeated using antibodies for GFP, β-actin, RNA Polymerase II Phospho Serine 5 [RNA polymerase II CTD repeat YSPTSPS (phospho ser5), Ab5131, Primary Ab 1:1000/2.5%BSA, 35 µL and 35 mL], and RNA Polymerase II (RNA polymerase II CTD repeat YSPTSPS, Ab26721, Primary Ab: 1:1000/2.5%BSA, 35 µL and 35 mL) with 2.5% bovine serum albumin (BSA)/TBST as the blocking buffer. Band intensity was quantified in Image Lab software and normalized to β-actin. Western blots were conducted both by myself and with the aid of Xiaohong Cui and Hannah Woolard.

RNA Sequencing

RNA Sequencing was conducted to determine the gene loci regulated by RPRD2. 10 tissue samples (5 HSV-RPRD2 and 5 HSV-GFP) from the third cohort (6 Day CSDS) were shipped to Genewiz (San Diego, CA) for RNA sequencing (Genomics from Azenta Life Sciences, n.d.).

High-throughput next-generation sequencing was used to enable RNA analysis through the

sequencing of complementary DNA (Kukurba & Montgomery, 2015). The RNA sequence library

was isolated by first conducting mRNA enrichment, mRNA fragmentation, and random priming

(Genomics from Azenta Life Sciences, n.d.). Next, the tissue strands were synthesized into

complementary DNA. The fragmented DNA was then exposed to end repair, 5'

phosphorylation, and dA-tailing. An adaptor was ligated to the adenine base overhang of the

DNA fragments and a polymerase chain reaction amplification was performed to amplify the

sequences (Kukurba & Montgomery, 2015). Sequence quality was evaluated and the reads

were trimmed to remove low quality adaptor sequences and nucleotides (Genomics from

Azenta Life Sciences, n.d.). The sequence reads were then mapped to the Mus Musculus

GRCm38 reference genome available on ENSEMBL using the STAR aligner v.2.5.2b–a splice

aligner that detects splice junctions and incorporates them to read sequences. Unique gene hit

counts were calculated using featureCounts from the Subread package v.1.5.2 in order to count

unique reads that fell within exon regions. After extraction, the gene hit counts were used for

downstream differential expression analysis. Using differential gene expression (DESeq2), a

comparison of gene expression between the provided tissue samples was performed. A volcano

plot was assembled in Graphpad Prism 9 using the log_2(fold change) of the normalized mean

hit counts for the gene and the -log_{10}(Wald test P value) where the nominal p-value = 1.85. This

process was conducted with the aid of Dr. Peter Hamilton.

Gene Ontology Analysis

A gene ontology analysis was conducted to analyze the biological processes affected by RPRD2. WebGestalt (WEB-based Gene SeT AnaLysis Toolkit), a functional enrichment analysis web tool, matched RPRD2 upregulated and downregulated gene transcripts to their corresponding function using the Benjamini-Hochberg false discovery rate < 0.05. Each geographic process was represented by the fold enrichment and portrayed geographically using Rstudio in which each plot point was colored by the $-log_{10}$(FDR P value) and sized by the number of corresponding genes. Gene Ontology analysis was conducted with the aid of Dr. Peter J. Hamilton and Kijoon Kim. Additionally, DropVis, a droplet-based single-cell RNA-seq, was used to determine discrete cell clusters that were highly enriched by RPRD2 upregulated and downregulated genes.

Perfusion

Perfusion was conducted on the fourth (6 Day CSDS) and fifth cohorts (No CSDS) following the SI and the EPM tests to fix the brain tissue. 0.3 mL of ketamine was administered in the abdominal cavity to induce anesthesia. 20-gauge 5 BD PrecisionGlide needles held down the rodent's paws and rib cage on an elevated styrofoam lid. A Scalp Vein Set attached to an Ismtec Masterflex Perfusion pump (4.8 mL/min) was injected into the rodent's left ventricle and the rodent was perfused with PBS until its liver lightened in color. The right atrium was snipped to allow blood flow. Then, PFA (32% stock EMgrade paraformaldehyde, diluted to 4%) was perfused until the rodent was rigid. Lastly, the system was flushed with PBS and the tools cleaned in 70% ethanol. The brain was extracted and refrigerated in a 5 mL Eppendorf tube

with 2.5 mL of PFA for 48 hours. Following this, the brain was transferred to a 15% sucrose

solution (15% sucrose in 1x PBS and 0.05% sodium azide) for 24 hours, a 30% sucrose solution

(30% sucrose in 1x PBS and 0.05% sodium azide) for 24 hours, and a 30% sucrose solution for

another 24 hours. Perfusions were conducted with the aid of Kijoon Kim.

Medium Spiny Neuron Morphology

Medium spiny neuron (MSN) morphology was conducted on Cohorts 4 (6 Day CSDS) and

5 (No CSDS) to analyze dendritic spine changes caused by RPRD2. Brain tissue was sliced on a

brain block with disposable single edge industrial razor blades in order to become nearer to the

NAc (ImageJ Wiki, n.d.). Sekundenkleber instant adhesive was used to glue the brain onto the

platform of a Leica VT1000S Vibratome and positioned so that the dorsal side of the brain faced

away from the bystander. The area of the NAc was estimated, and roughly the prefrontal cortex

and cerebellum were sliced away before tissue sectioning. The remaining brain was placed in

PBS so that it was covered entirely and a personna super blade was used to slice 40 μm of

tissue. A paint brush was used to capture each slice and set each NAc section of the brain on a

RITE-ON micro slide (3 x 1 in, 1.1-1.3 mm thick). Once the sections dried on the slide, each

tissue slice was covered with one drop of NucBlue Fixed Cell Stain ReadyProbes reagent and

each slide was covered with ProLong Glass Antifade Mountant (about 10 slices per slide, 2-3

slides per brain). Any remaining brain sections were removed with acetone. The slides were

placed in a 4°C refrigerator overnight and imaged the next day with Keyence BZ-X810.

Immersion oil type HF was used for magnifications 60x or higher. MSN morphology was conducted on tissue samples that had the most fluorescence and clarity, as they indicated the best targeted NAc during stereotaxic surgery. Selection criteria also included the ability to observe dendrites and not simply a tract of axons. The selected tissue samples were chosen with the aid of Natalie Truby, who was intimately familiar with the NAc, but an objective bystander in regard to this experiment. Neurons were traced in (Fiji Is Just) ImageJ.

Statistical Analysis

Data were analyzed using GraphPad Prism Software. Three-way Analysis of variance (ANOVA) and two-tailed unpaired t tests were run to compare the results of the SI test, thigmotaxis, and EMP test within groups ($p \leq 0.05$).

Results

As stated above, the first cohort of mice did not experience CSDS to act as a control cohort and to understand the consequence of HSV-RPRD2 delivery to the NAc in the absence of stress **(Figure 1.A)**. The second cohort of mice experienced CSDS for 10 minutes, twice a day, for 5 days **(Figure 1.B)**. The third **(Figure 1.C)** and fourth **(Figure 1.D)** cohort experienced CSDS for 11 minutes, twice a day, for 6 days. NAc tissue samples from the third cohort were processed for RNA sequencing. Data from the fourth cohort was originally intended to conduct MSN morphology; however, too much time may have passed between viral delivery of RPRD2 and the analysis of the tissue which led to GFP no longer being visible. Despite this, behavioral analysis was still conducted and used to further power the results. The fifth cohort did not experience CSDS and was instead used for MSN morphology analysis **(Figure 1.E)**.

To confirm that HSV-RPRD2 was indeed virally overexpressed in MSNs of the NAc, a Western blot was conducted retroactively on the membranes obtained from mice in Cohort 1 (No CSDS) and Cohort 2 (5 Day CSDS). This study is still ongoing in order to achieve significant results and confirm the relative expression of HSV-RPRD2 in comparison to HSV-GFP. This process is led by Hannah Woolard.

Social behavior was not significantly impacted by RPRD2.

A social interaction (SI) test was conducted to measure social behavior of mice with viral overexpression of RPRD2 in the NAc both in the absence and in the presence of a novel CD1

mouse (File & Hyde, 1978). Social behavior was quantified by the seconds a male C57BL/6J mouse spends in the 18 x 25 cm dimensions of the interaction zone of an SI area; less time spent in the interaction zone in the presence of a novel CD1 mouse indicates a decrease in social behavior.

Overall, one-way ANOVA did not show a significant effect on the time spent in the interaction zone of an SI test. Unstressed RPRD2 mice in Cohort 1 (No CSDS) in the presence of an aggressive CD1 male mouse did not spend a significant amount of time in the interaction zone (p = 0.7950) in comparison to GFP mice **(Figure 2.A)**. Amongst stressed mice from Cohort 2 (5 Day CSDS), Cohort 3 (6 Day CSDS), and Cohort 4 (6 Day CSDS), the same effect was observed (p = 0.6896) **(Figure 2.B)**. Data from the first four cohorts were combined and no significant difference was observed between the RPRD2 and GFP mice (p = 0.5732), regardless of an aggressor CD1 mouse **(Figure 2.C)**. Collectively, this data indicates that viral overexpression of RPRD2 within the NAc of unstressed or stressed mice does not impact social behavior.

Increased levels of RPRD2 indicates an increase in anxiety-like behavior in male mice.

Elevated plus maze (EPM) test was conducted to specifically measure anxiety-like behavior in mice with viral overexpression of RPRD2 (Bailey & Crawley, 2009; Kraeuter et al., 2019; Rodgers & Dalvi, 1987). Less time spent in the open arms of the EPM–and thus more time in the closed arms–over the course of 5:00 minutes correlates with increased physiological stress and anxiety-like behavior.

From this paradigm, unpaired t tests showed a significant effect on time spent in the open arms of an EPM test between stressed RPRD2 and GFP mice. Without exposure to chronic stress, unpaired t tests did not reveal a significant effect on time spent in the open arms for mice in Cohort 1 (No CSDS) **(Figure 3.A)**; however, a downward trend was observed in which RPRD2 mice spent less time in the open arms than GFP mice (p = 0.2042). Data from chronically stressed RPRD2 mice in Cohort 2 (5 Day CSDS), Cohort 3 (6 Day CSDS), and Cohort 4 (6 Day CSDS) did portray significantly less time in the open arms (p = 0.0484) than GFP mice **(Figure 3.B)**. In combining Cohorts 1-4 EPM data, RPRD2 mice spent significantly less time in the open arms (p = 0.0169) than did GFP mice, indicating anxiety-like behaviors in mice virally overexpressed with RPRD2 **(Figure 3.C)**.

To further enforce the importance of the results of the EPM paradigm, thigmotaxis was retroactively measured using the SI test data to determine the tendency of mice to remain close to the walls. Decreased time spent in the center zone of the SI arena (17 x 32 cm) in the absence of an aggressor CD1 mouse indicated increased fear or anxiety (Simon et al., 1994). In general, one-way ANOVA did not show a significant effect on thigmotaxis. Unstressed RPRD2 mice in Cohort 1 (No CSDS) did not spend a significantly different amount of time in the center zone (p = 0.8041) in the absence of an aggressor CD1 mouse in comparison to GFP mice **(Figure 4.A)**. Data from chronically stressed RPRD2 mice in Cohort 2 (5 Day CSDS), Cohort 3 (6 Day CSDS), and Cohort 4 (6 Day CSDS) did display a trend of less time spent in the center zone (p = 0.1130) in comparison to the GFP mice; however, significance was not attained **(Figure 4.B)**. In combining Cohorts 1-4 EPM data, RPRD2 mice spent less time in the center zone (p = 0.1247) in comparison to the GFP mice **(Figure 4.C)**. This trend of increased thigmotaxis seen further

supports anxiety-like behaviors in mice virally overexpressed with RPRD2, but must be cautiously interpreted as the behavioral effect did not reach significance.

The impact of RPRD2 on RNA polymerase II phospho ser5 levels.

After quantifying the behavioral impact of RPRD2 overexpression, the molecular impact of RPRD2 was quantified by assessing levels of RNA polymerase II phospho ser5. As RPRD proteins were implicated in decreasing phosphorylation of serines at position 5 of the carboxyl-terminus domain of RNA Polymerase II, heightened levels of RPRD2 protein might lower levels of phospho ser5 and would further connect these results to a decrease in transcriptional activity in this brain area.

Overall, unpaired t tests did not show a significant effect in RNA polymerase II phospho ser5 activity, indicated by the normalization factor. The normalization factor was calculated by dividing the RNA polymerase II phospho ser5 adjusted total band volume–from the Western blot images–by the β-actin adjusted total band volume **(Figure 5.A)**. The HSV-RPRD2 normalization factor values in each membrane were averaged and set as 1 for the data set to allow comparison between membranes.

Although no significance was reached, tissue samples from unstressed RPRD2 mice in Cohort 1 (No CSDS) did reveal slightly decreased levels of RNA polymerase II phospho ser5 (p = 0.3287) in comparison to the GFP mice **(Figure 5.B)**. Stressed RPRD2 mice in Cohort 2 (5 Day CSDS) also revealed a similar, stronger trend (p = 0.2712) **(Figure 5.C)**. Cohort 3 (6 Day CSDS) data was unavailable as the tissue samples were sent for RNA sequencing, and Cohort 4 (6 Day

CSDS) data was unavailable as the tissue samples were unsuccessfully used to analyze MSN

morphology. Additionally, Cohort 1 (No CSDS) and Cohort 2 (5 Day CSDS) combined

normalization factor data ($p = 0.0745$) revealed a strong downward trend in levels of RNA

polymerase II phospho ser5 for RPRD2 mice in comparison to GFP mice **(Figure 5.D)**. While our

individual cohorts were likely not powered sufficiently to detect a significant decrease in RNA

polymerase II phospho ser5 levels mediated by viral overexpression of RPRD2, combining these

cohorts enabled more robust detection of the regulatory role of RPRD2 on RNA polymerase II.

These data suggest that RPRD2 likely does act to dephosphorylate serines at position 5 on the

CTD of RNA polymerase II in the neurons of the NAc, though further analyses will be required to

achieve a significant result.

Total levels of RNA polymerase II were measured to determine the total effect RPRD2

may have on the CTD on RNA polymerase II. Measuring the total RNA polymerase II via a

Western blot proved difficult as its molecular mass was very similar to that of RNA Pol II

phospho ser5 (220 kD for the former, 250 kD for the latter). Despite this, the normalization

factor was calculated by dividing the RNA polymerase II adjusted total band volume–from the

Western blot images–by the β-actin adjusted total band volume **(Figure 6.A)**. The HSV-RPRD2

normalization factor values in each membrane were averaged and set as 1 for the data set to

allow comparison between membranes.

Tissue samples from unstressed RPRD2 mice in Cohort 1 (No CSDS) did not show a

significant effect on total RNA polymerase II levels ($p = 0.7598$) in comparison to the GFP mice

(Figure 6.B). Stressed RPRD2 mice in Cohort 2 (5 Day CSDS) did reveal a slight downward trend

of RNA polymerase II levels, but the trend was not significant ($p = 0.1488$) **(Figure 6.C)**. Cohort 3

(6 Day CSDS) data was unavailable as the tissue samples were sent for RNA sequencing, and

Cohort 4 (6 Day CSDS) data was unavailable as the tissue samples were unsuccessfully used to

analyze MSN morphology. Combined normalization factor data from Cohort 1 (No CSDS) and

Cohort 2 (5 Day CSDS) did not reveal significance (p = 0.4370) **(Figure 6.D)**. These data suggest

that the observed effect of RPRD2 decreasing phosphorylation of the CTD of RNA polymerase II

is not due to changes in the total amount of RNA polymerase II, and further solidifies its effect

on the dephosphorylation of serine at position 5 on the CTD of RNA polymerase II in the

neurons of the NAc.

RPRD2 primarily impacts genes that are typically highly enriched in fibroblast and ependymal

cell types.

We next explored the molecular impact of RPRD2 on transcription in the NAc. We

hypothesized that RPRD2 may regulate the expression of key gene loci via its

dephosphorylation and subsequent regulation of RNA polymerase II. Tissue samples from

Cohort 3 (6 Day CSDS) were subjected to RNA sequencing (see Methods) and DEGs were

generated across the HSV-RPRD2 and HSV-GFP groups to explore the gene loci potentially

regulated by RPRD2. A volcano plot was assembled and analyzed (nominal p-value threshold set

to = $-log_{10}(1.85)$) **(Figure 7)**. RPRD2 upregulated genes were colored yellow, and RPRD2

downregulated genes were colored blue.

The most significantly upregulated gene identified was Slc47a1. DropVis data revealed

that this gene, as well as many other upregulated DEGs, is highly enriched in fibroblast cells

(Figure 8.A). Contrastingly, many dynein-related genes were significantly downregulated, such as Dnah12. Using the gene loci identified through the RNA sequence, DropVis data revealed that RPRD2 primarily downregulates genes highly enriched in ependymal cells **(Figure 8.B)**. Given that HSVs exclusively infect neurons, it is unclear whether viral overexpression of RPRD2 in NAc neurons indirectly induces these DEGs within the aforementioned non-neuronal cell types or if RPRD2 is directly responsible for regulating these DEGs in the infected neurons, which under basal conditions are enriched in fibroblast or ependymal cells.

RPRD2 may decrease microtubule transport in neurons within the NAc.

Using the genes identified from the RNA sequencing data, a gene ontology analysis was conducted to analyze the biological processes affected by overexpression of RPRD2. GO over-representation analysis revealed that the common upregulated GO terms were related to extracellular matrix organization, tube development, and embryo development **(Figure 8.C)**. GO over-representation analysis also revealed that the common downregulated GO terms were related to microtubule-based movement, cilium organization, and organelle assembly **(Figure 8.D)**. Amongst all terms, microtubule-based movement had the highest Fold Enrichment Value and the most red $-log_{10}$(FDR P value).

RPRD2 may decrease dendritic branches of MSNs in the NAc.

We hypothesized that viral delivery of RPRD2 to the NAc would decrease transcription at key genes, and we identified microtubule-related genes as the top downregulated transcripts. We next aimed to explore what consequence this might have on the cellular morphology of MSNs, the principle neuronal cell-type in the NAc. MSN morphology was observed by viewing the amount of neuronal dendritic branching. We hypothesized that diminished MSNs may indicate susceptible, anxiety-like behavior in mice following CSDS. Upon observing images of MSNs in the NAc of mice from Cohort 5 (No CSDS) in (Fiji Is Just) ImageJ, it appeared that there was less dendritic branching in neurons injected with viral overexpression of HSV-RPRD2 **(Figure 9.A)** than those with HSV-GFP **(Figure 9.B)**. However, this is a preliminary observation and further analysis is needed to definitively determine the significance of this observation.

Figure 1.

A.
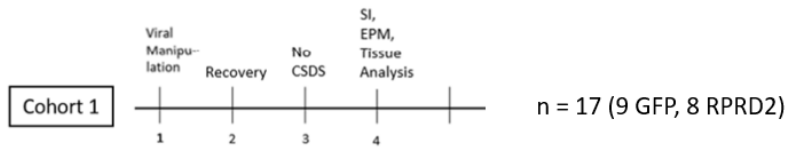
B.
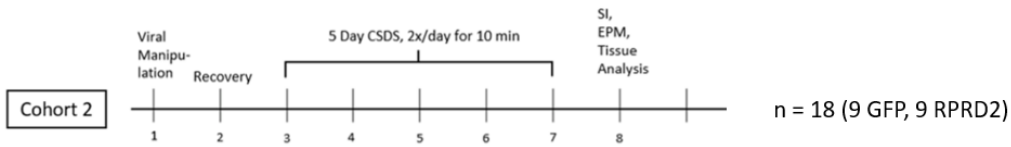
C.
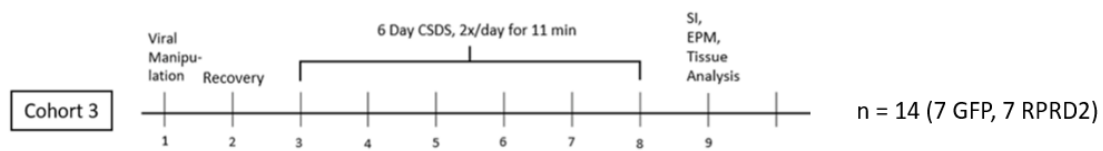
D.
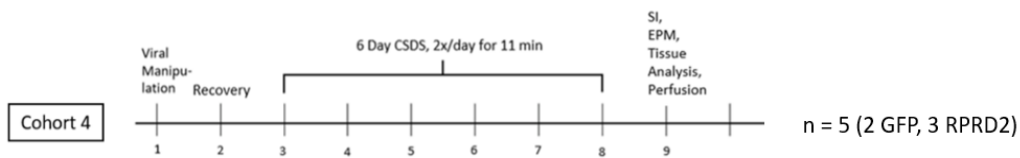
E.
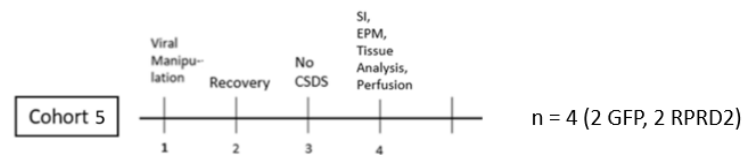
Figure 1: *Timeline of the Chronic Social Defeat Stress for each cohort.*

Figure 2.

A.
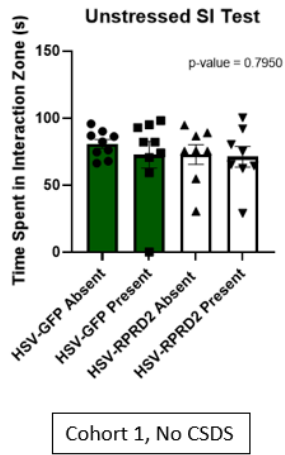
B.
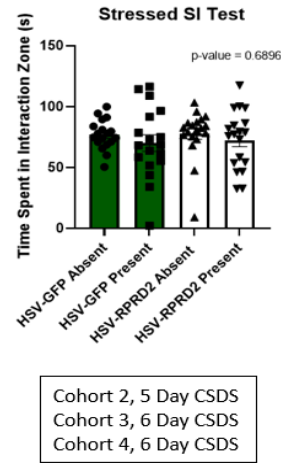
C.
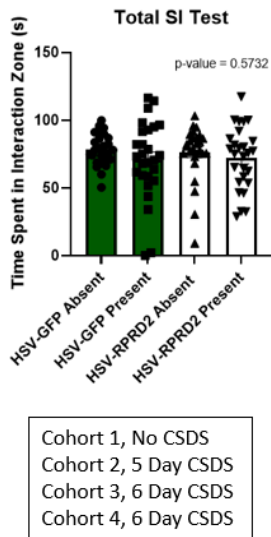
Figure 2: *Amongst all cohorts, time spent in the interaction zone during the SI test did not yield statistically significant results.* A) With or without the presence of a CD1 aggressor mouse, the groups within Cohort 1 (No CSDS) did not portray a significant difference in the time spent in the interaction zone. B) Stressed mice in Cohort 2 (5 Day CSDS), Cohort 3 (6 Day CSDS), and Cohort 4 (6 Day CSDS) did not significantly reveal a difference in time spent in the interaction zone. C) All mice across Cohorts 1-4 did not portray a significant difference in the time spent in the interaction zone within the groups. Symbols represent mean ± SEM.

Figure 3.

A.

Unstressed Open Arm EPM Test

p-value = 0.2042
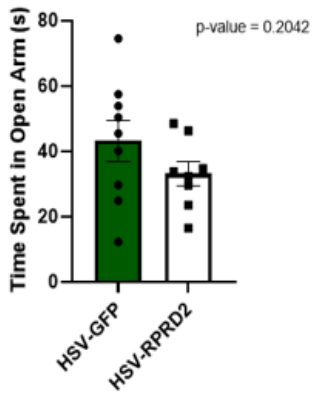
Cohort 1, No CSDS

B.

Stressed Open Arm EPM Test

p-value = 0.0484
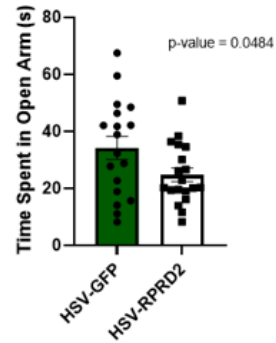
Cohort 2, 5 Day CSDS
Cohort 3, 6 Day CSDS
Cohort 4, 6 Day CSDS

C.

Total Open Arm EPM Test

p-value = 0.0169
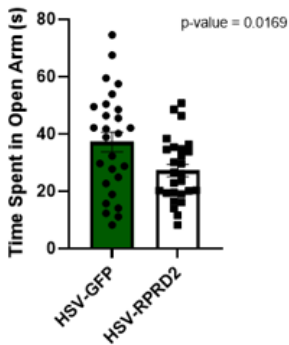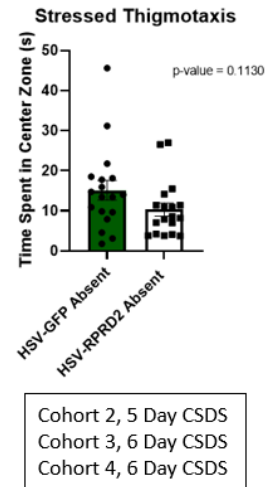
Cohort 1, No CSDS
Cohort 2, 5 Day CSDS
Cohort 3, 6 Day CSDS
Cohort 4, 6 Day CSDS

Figure 3: *Amongst mice exposed to CSDS, time spent in the open arms of the EPM revealed a downward trend.* A) Unstressed mice with overexpression of RPRD2 in Cohort 1 (No CSDS) spent less time in the open arms of the EPM than GFP mice, but the trend is not significant. B) Stressed RPRD2 mice in Cohort 2 (5 Day CSDS), Cohort 3 (6 Day CSDS), and Cohort 4 (6 Day CSDS) revealed significantly less time spent in the open arms than GFP mice. C) All RPRD2 mice across Cohorts 1-4 displayed significantly less time spent in the open arms than GFP mice. Symbols represent mean ± SEM.
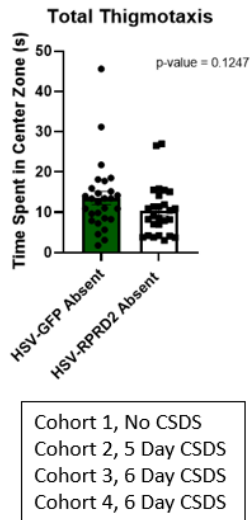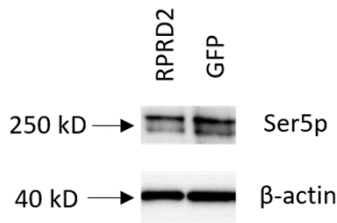
Figure 4.

A.
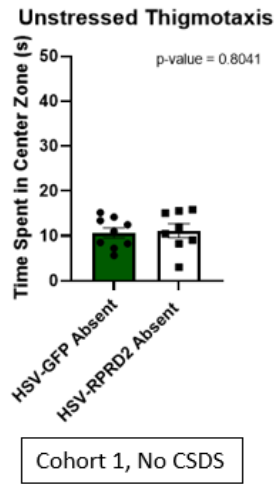
B.

C.

Figure 4: *Amongst all cohorts, thigmotaxis yielded a downward trend in stressed mice with viral overexpression of RPRD2.* A) Unstressed mice with viral overexpression of RPRD2 in Cohort 1 (No CSDS) did not reveal a significant difference in the amount of time spent in the center zone in the absence of a CD1 aggressor mouse in comparison to GFP mice. B) Stressed RPRD2 mice in Cohort 2 (5 Day CSDS), Cohort 3 (6 Day CSDS), and Cohort 4 (6 Day CSDS) revealed a trend of less time spent in the center zone in comparison to GFP mice. C) All RPRD2 mice across Cohorts 1-4 displayed a downward trend of time spent in the center zone in the absence of a CD1 aggressor mouse in comparison to GFP mice. Symbols represent mean ± SEM.
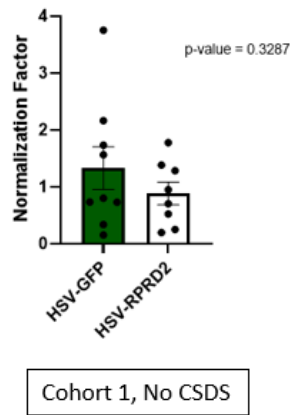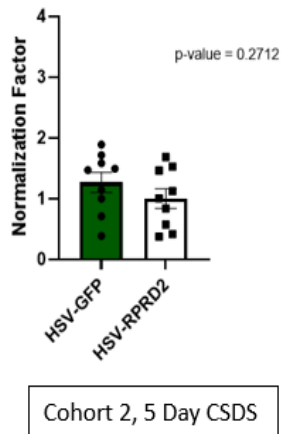
Figure 5.

A.

B.

Unstressed Phospho Ser5 Levels

p-value = 0.3287

Cohort 1, No CSDS

C.

D.

Stressed Phospho Ser5 Levels

p-value = 0.2712

Cohort 2, 5 Day CSDS

Total Phospho Ser5 Levels

p-value = 0.0745

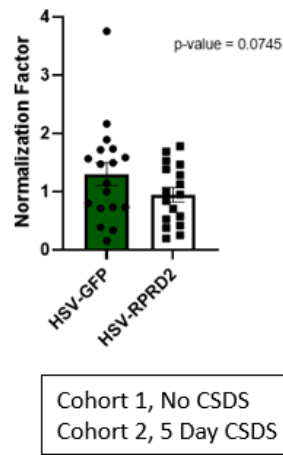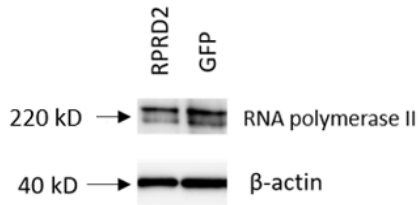Cohort 1, No CSDS
Cohort 2, 5 Day CSDS

Figure 5: *Normalized RNA Polymerase II Phospho Ser5 levels revealed a downward trend in RPRD2 mice.* A) A representative blot of RNA Polymerase II Phospho Ser5 levels showed less Ser5p (lighter band on Western blot) in RPRD2 mice than GFP mice. B) Unstressed RPRD2 mice of Cohort 1 (No CSDS) revealed a downward trend of Ser5p levels in comparison to GFP mice. C) Stressed RPRD2 mice of Cohort 2 (5 Day CSDS) revealed a downward trend of Ser5p levels. D) All mice with viral overexpression of RPRD2 in Cohorts 1-2 revealed a downward trend in Ser5p levels, but no significance was reached. Symbols represent mean ± SEM.
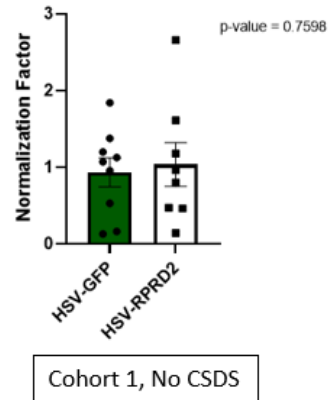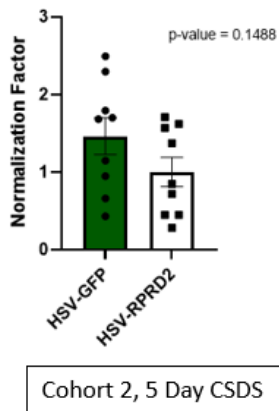
Figure 6.

A.

B.

Unstressed RNA Polymerase II Levels

Cohort 1, No CSDS

C.

Stressed RNA Polymerase II Levels

Cohort 2, 5 Day CSDS

D.

Total RNA Polymerase II Levels

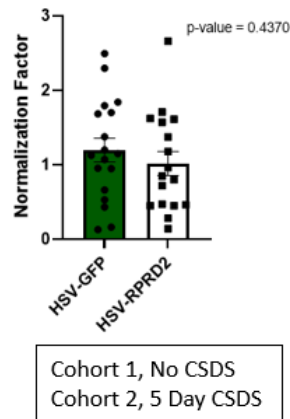Cohort 1, No CSDS
Cohort 2, 5 Day CSDS

Figure 6: *Normalized RNA Polymerase II levels revealed a downward trend in RPRD2 mice.* A) A representative blot of total RNA polymerase II levels showed less RNA polymerase II (lighter band on Western blot) in RPRD2 mice than GFP mice. B) Unstressed RPRD2 mice of Cohort 1 (No CSDS) revealed a downward trend of RNA polymerase II levels in comparison to GFP mice. C) Stressed RPRD2 mice of Cohort 2 (5 Day CSDS) revealed a downward trend of RNA polymerase II levels. D) All mice with viral overexpression of RPRD2 in Cohorts 1-2 revealed a downward trend in RNA polymerase II levels, but no significance was reached. Symbols represent mean ± SEM.
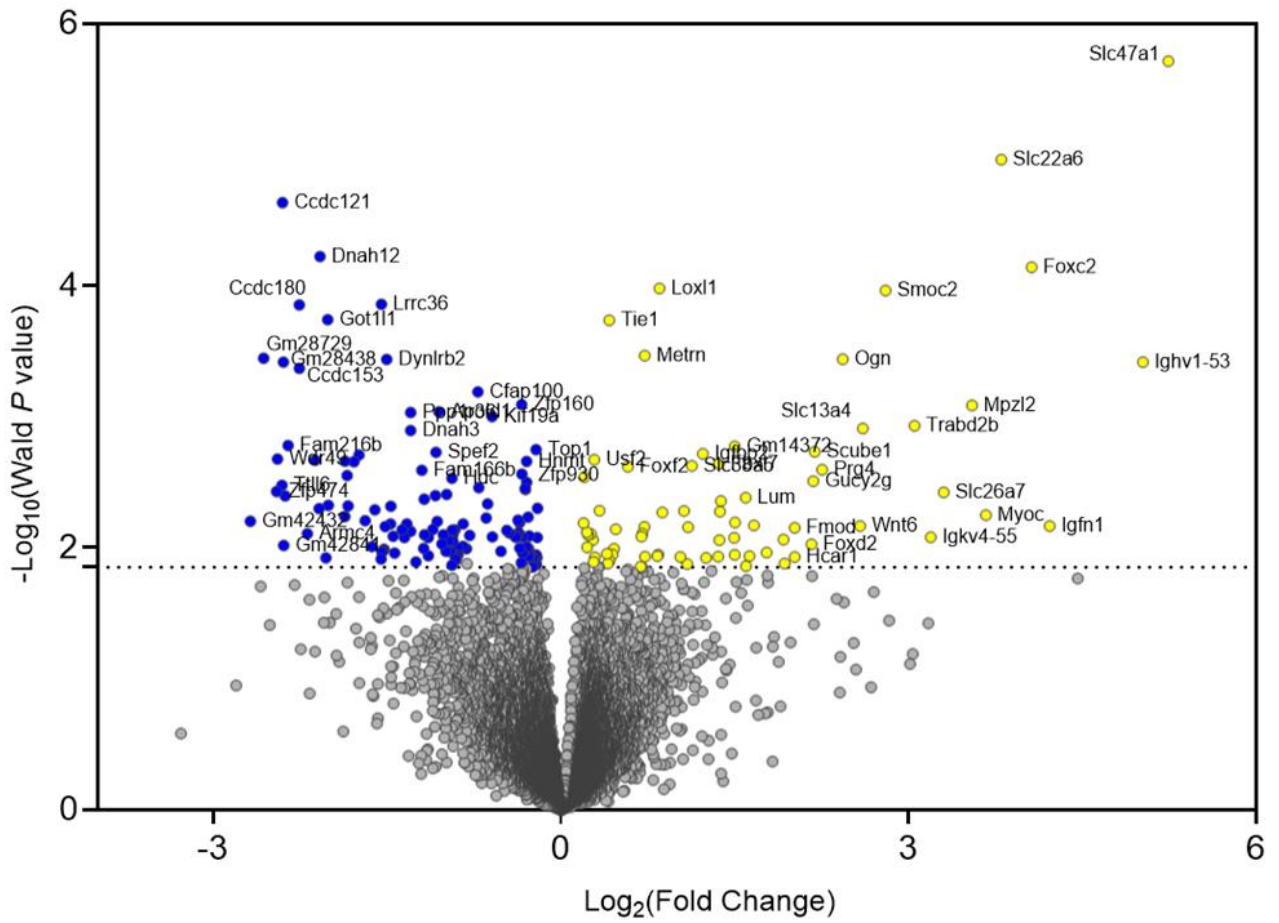
Figure 7.

Figure 7: *Volcano plot from RNA sequence displaying RPRD2 upregulated (yellow) and downregulated (blue) genes.*

Figure 8.

A.
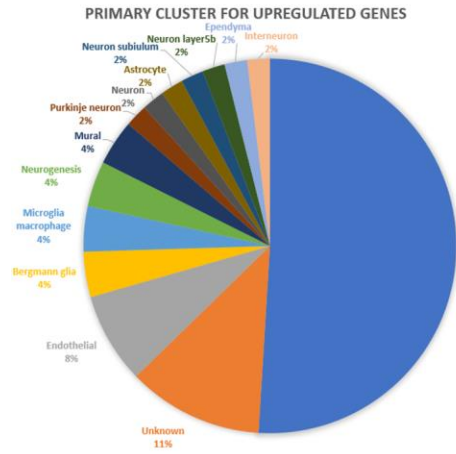
B.
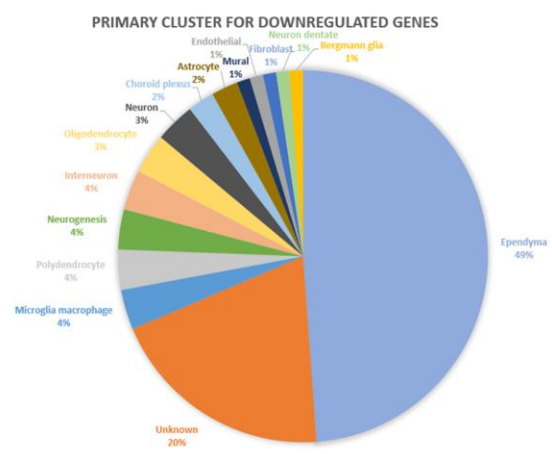
C.
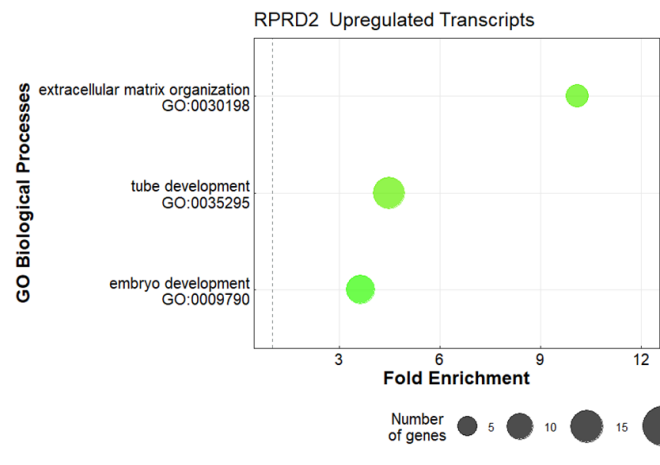
D.
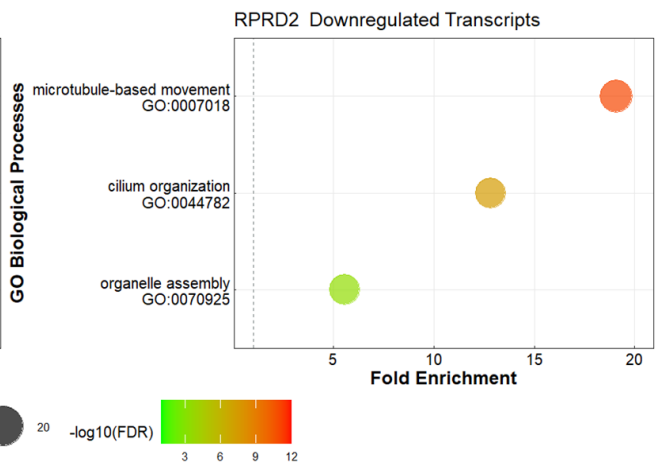
Figure 8: *Male mice with RPRD2 overexpression displayed distinct upregulated and downregulated targets.* A) Pie chart depicting discrete cell clusters that were highly enriched by RPRD2 upregulated genes. B) Pie chart depicting discrete cell clusters that were highly enriched by RPRD2 downregulated genes. C) Visualization of key gene ontology functions among the upregulated RPRD2 gene list. D) Visualization of key gene ontology functions among the downregulated RPRD2 gene list.

Figure 9.

A.
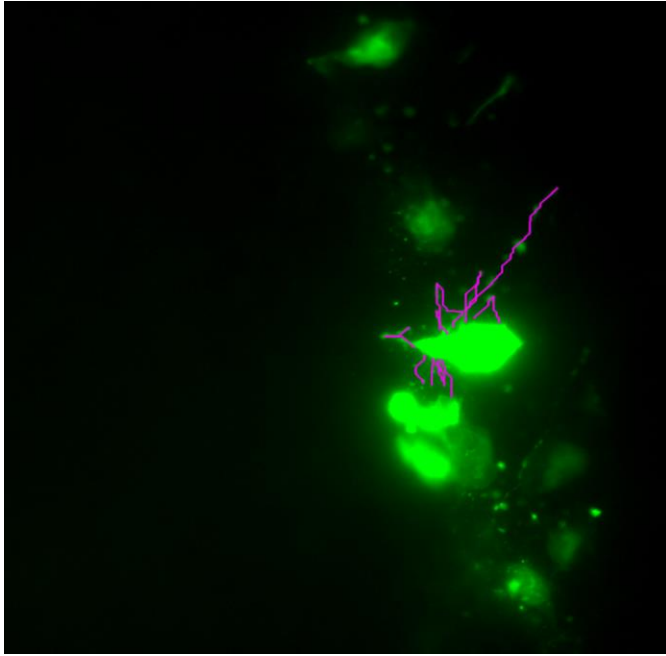
B.
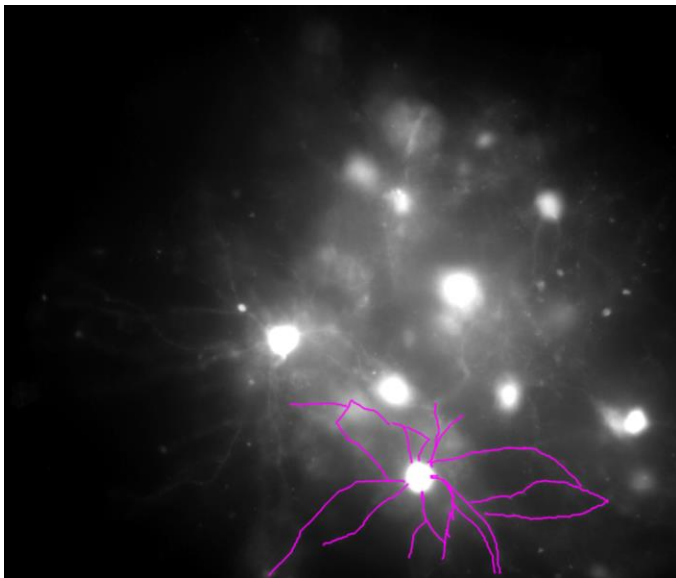
Figure 9: *HSV-RPRD2 MSNs appear to be less branched than HSV-GFP MSNs.* A) Image of RPRD2 MSN. B) Image of GFP MSN.

Discussion

Anxiety-like behavior following increased levels of RPRD2

Earlier work from our laboratory identified RPRD2 differentially expressed in the brain of mice stratified in terms of their phenotypic response to chronic stress (Hamilton et al., 2020). RPRD2 protein was elevated in the NAc of stress resilient animals–mice that display less behavioral abnormalities and more successful adaptation to stressors. To test social behavior, a social interaction test was conducted; less time spent in the interaction zone in the presence of an aggressor CD1 mouse indicates a decrease in social behavior (File & Hyde, 1978). As seen in the figures above, social interaction was not affected by chronic social defeat stress following elevated levels of RPRD2. There were no significant differences in time spent in the interaction zone between groups. Therefore, viral overexpression of RPRD2 within the NAc of unstressed or stressed mice did not impact social behavior.

Behavioral data was also collected from an EPM test. The EPM test is a well-established paradigm measuring anxiety-like behavior in mice (Bailey & Crawley, 2009). This test takes advantage of mice's natural tendency to avoid open areas. Less time spent in the open arms of the EPM–and thus more time in the closed arms–correlates with increased physiological stress. As seen in the data above, stressed C57BL/6J mice, and not unstressed C57BL/6J mice, with viral overexpression of RPRD2 spent significantly less time in the open arms of the EPM than did GFP mice. This indicated that elevated levels of RPRD2 specifically engendered stress-induced anxiety-like behavior.

Distance (cm) and velocity (cm/s) moved in the EPM paradigm was also assessed to determine if the decreased time spent in the open arms was associated with reduced locomotion in general amongst mice with viral overexpression of RPRD2 in comparison to the control. Reduced locomotion could indicate that RPRD2 mice chose a location in the EPM and remained in that location for the remaining testing period. Data collected revealed that unstressed and stressed RPRD2 and GFP mice moved roughly equal distances and at equal velocity (not shown). Thus, RPRD2 mice expressed no change in locomotion in comparison to GFP mice, and truly spent less time in the open arms of the EPM.

To further explore RPRD2's correlation to anxiety-like behavior, thigmotaxis was retroactively measured using the SI test data to determine the tendency of mice to remain close to the walls. Decreased time spent in the center zone in the absence of an aggressor CD1 mouse indicated increased fear or anxiety (Simon et al., 1994). Specifically, chronically stressed mice with viral overexpression of RPRD2, and not unstressed mice, revealed a downward trend of less time spent in the center zone. This trend of increased thigmotaxis upon exposure to chronic stress indicates anxiety-like behaviors in mice virally overexpressed with RPRD2, as well as the results of the EPM test.

As discussed above, evidence suggests that resilient mice have higher levels of RPRD2 protein within the NAc in comparison to susceptible mice when exposed to CSDS (Hamilton et al., 2020; Wendelmuth et al., 2020). However, the data presented above indicates that RPRD2 is associated with anxiety-related behaviors when mice are exposed to CSDS. Rejection of the initial assumption of RPRD2's behavioral role was prompted by the difference in the two studies' methodology. In the experiment conducted by Hamilton et al., the mice were exposed

to stress and a proteomic analysis revealed elevated RPRD2 in the NAc (Hamiton et al., 2020). However, the approach used in this experiment first began with viral overexpression of RPRD2, then exposure to CSDS, and finally an analysis of the NAc. The varying sequence of events and adjusted levels of RPRD2 could be underlying factors for the difference seen in the behavioral role of RPRD2 in the NAc.

These collective novel findings suggest that viral overexpression of RPRD2 plays a role in governing anxiety-related behaviors. This solicited further questions as to the mechanistic impact of this protein in the NAc. In discerning the impact of RPRD2 overexpression with the NAc, RPRD2 may be targeted in order to develop effective pharmacotherapies for those with anxiety disorders. The molecular impact of viral overexpression of RPRD2 needed to be investigated, which led to exploring the effect of RPRD2 on RNA Polymerase II Phospho Ser5 activity levels.

Effect of RPRD2 on S5p levels

RPRD proteins have been implicated in decreasing phosphorylation of serines at position 5 of the carboxyl-terminus domain of RNA Polymerase II. Heightened levels of RPRD2 protein may lower levels of phospho ser5 and thus decrease transcriptional activity of RNA polymerase II (Ni et al., 2011; Ali et al., 2019). Following a Western blot, RNA Polymerase II Phospho Ser5 levels (normalized to β-actin) revealed a strong downward trend in RPRD2 mice in comparison to GFP mice and sufficient detection of the regulatory role of RPRD2 on RNA polymerase II. This trend indicated that increased levels of RPRD2 decreased phosphorylation of serines at position

5 on the CTD of RNA polymerase II in the neurons of the NAc, in accordance with my

hypothesis. This data is consistent with previous findings conducted on RPRD proteins.

Total levels of RNA polymerase II were measured as well to determine the total effect

RPRD2 may have on the CTD on RNA polymerase II. Measuring the total RNA polymerase II via a

Western blot proved difficult as its molecular mass was very similar to that of RNA Pol II

phospho ser5 (220 kD for the former, 250 kD for the latter). Between antibodies used to target

these variables, the membranes were thoroughly washed to avoid any band crossover or

residue from the previous target. These data suggest that RPRD2 does not appear to impact

total protein levels of RNA polymerase II, and further solidifies its effect on the

dephosphorylation of serine at position 5 on the CTD of RNA polymerase II in the neurons of

the NAc.

As stated above, increased levels of RPRD2 decrease phosphorylation of serines at

position 5 on the CTD of RNA polymerase II in the neurons of the NAc. This may induce

downstream effects on transcription of certain genes within the NAc and downregulate their

expression. Manipulation of even a single gene can profoundly affect behavior (Robinson et al.,

2008). Genome sequencing can detect genomic variation and aid in understanding how genetic

information influences brain circuits that mediate behavior (Robinson et al., 2008).

Primary cluster types and biological processes impacted by RPRD2

It has been previously shown that changes in the NAc can affect psychiatric disorders

such as anxiety disorders and a host of others (Mavridis, 2015). High-throughput next

generation sequencing was conducted to enable RNA analysis in order to discern more exact changes in the NAc and how those changes may be influencing those with anxiety-like behavior.

The most significantly upregulated gene identified was Slc47a1. DropVis data revealed that this gene, as well as many other upregulated DEGs, is highly enriched in fibroblast cells. Fibroblast cells can be found in perivascular spaces, meninges, and choroid plexus of the brain and spinal cord (Dorrier et al., 2022). They provide structural support to connective tissues by secreting extracellular matrix components, produce cytokines and growth factors, assist in angiogenesis, and respond to mechanical stress by remodeling tissue. Contrastingly, many dynein-related genes were significantly downregulated, such as Dnah12. Using the gene loci identified through the RNA sequence, DropVis data revealed that RPRD2 primarily downregulates genes highly enriched in ependymal cells. Ependymal cells are responsible for transporting electrolytes between cerebral spinal fluid and brain parenchyma, and may contribute to osmotic control through cotransporters (Daroff et al., 2014; Meunier & Spassky, 2020).

As stated previously, it is unclear whether viral overexpression of RPRD2 in NAc neurons indirectly or directly induces these DEGs. Given that HSVs exclusively infect neurons, I predict that viral overexpression of RPRD2 more likely indirectly regulates these DEGs enriched in fibroblast or ependymal cell types by a secondary mechanism; yet, this prediction should be explored more in the future.

A gene ontology analysis was conducted to further analyze the biological processes affected by overexpression of RPRD2 in the NAc. GO over-representation analysis revealed that, amongst all terms, microtubule-based movement was the biological process least likely due to

chance, and thus most significant. This suggests that viral overexpression of RPRD2 regulates key genes associated with microtubule transport, and downregulation of microtubule related genes along neurons in the NAc may be an underlying mechanism contributing to the development of anxiety disorders.

Changes in MSN morphology

Changes in microtubule expression have been implicated in neuropsychiatric disorders (Marchisella et al., 2016). As microtubules are capable of polymerizing into dendritic spines, and as microtubule-based movement is most significantly downregulated in neurons in the NAc, this brings into question the role of RPRD2 in regulating dendritic complexity and function of NAc MSNs (Dent, 2017). Previous studies revealed that diminished MSNs may indicate susceptible, anxiety-like behavior in mice following CSDS (Francis & Lobo, 2017). MSN morphology was observed by viewing the amount of neuronal dendritic branching with a simple neurite tracer, and it appeared that there was less dendritic branching in neurons injected with viral overexpression of HSV-RPRD2 than those with HSV-GFP.

Decreased dendritic spine density and dendritic arborization–branching at the end of a nerve fiber–have been largely associated with neurological diseases, specifically with depression and schizophrenia in response to chronic stress, both of which are comorbid with anxiety disorders (Anxiety & Depression Association of America, 2021; Marchisella et al., 2016). Loss of synapses due to these reduced arborizations leads to disrupted feedback loops and reduced adaptation to stressors (Duman & Canili, 2015). Collectively, these findings indicate

that decreased MSN morphology is associated with stressed-induced anxiety-like behaviors. Thus, RPRD2-mediated regulation of RNA polymerase II phosphorylation may preferentially affect genes involved in microtubule-based movement, which consequently inhibits the dendritic complexity and function of NAc MSNs; yet, additional analysis is needed to definitively confirm the decreased effect of viral overexpression of RPRD2 on MSN dendritic branching within the NAc.

Future Aims and Conclusions

Further investigation is needed in order to fully understand the implications of this data. Given that women are twice as likely to be affected with Generalized Anxiety Disorder, Panic Disorder, and Specific Phobias as men, it is important to note that very different behaviors and molecular pathways may be affected by RPRD2 in female mice than in male mice (Anxiety & Depression Association of America, 2021). As seen in Herbison et al., medium to high chronic stress exposure during adolescence predicted depression and anxiety symptoms in females, and high stress in early stages of pregnancy contributed to male depression and anxiety symptoms as well (Herbison et al., 2017). Therefore, female C57BL/6J mice should be invested using the same conditions as the studied male cohorts.

Due to lack of time and resources, HSV was used as a viral vector to target neurons. An accelerated defeat paradigm was conducted as HSV expression in neurons is only evident for 3-7 days. The ongoing study to confirm that HSV-RPRD2 was indeed virally overexpressed in MSNs of the NAc should be concluded and the results analyzed. In the future, adeno-associated

virus (AAV) may be used in order to virally deliver RPRD2 to the NAc. Following stereotaxic

surgery, expression of AAV-RPRD2 may be detectable anywhere from 1-4 weeks, allowing a full

10 days of CSDS (Stoica et al., 2013). Use of AAV would ensure RPRD2's viral overexpression in

MSNs of the NAc when conducting behavioral tests and further power our results.

Although there appeared to be less dendritic branching in neurons virally overexpressed

with RPRD2, a Sholl analysis must be conducted in the future in order to solidify this

observation and reduce observer bias. A Sholl analysis can quantify neuronal dendritic

complexity and truly determine if MSN morphology was blunted due to viral overexpression of

RPRD2 (Binley et al., 2014). As MSN morphology was not seen with Cohort 4 (6 Day CSDS) due

to GFP no longer fluorescing, further investigation is needed in order to determine if both CSDS

and a MSN morphology can be conducted while maintaining the pervasiveness of RPRD2.

Previous studies have shown decreased glutamatergic transmission of prefrontal cortex-NAc

synapses and decreased strength of hippocampus-NAc synapses of mice expressing depression-

like behavior following CSDS (Bagot et al., 2015; LeGates et al., 2018). Thus, it would be

interesting to investigate how MSN morphology changes along those synapses after CSDS.

In regard to gene loci, further studies should be conducted to explore the connections

between RPRD2 and its upregulated and downregulated genes. Attention may be best placed

on genes expressed in fibroblast and ependymal cell types. An in-depth motif analysis may be

beneficial in order to predict transcription factor binding events and a mechanistic pathway for

RPRD2 in the NAc. Additionally, further analysis should be conducted to achieve a significant

effect on RPRD2's dephosphorylation of serines at position 5 on the CTD of RNA polymerase II

in the neurons of the NAc.

In conclusion, I expanded on previous studies conducted on male mice revealing that resilient mice had higher levels of RPRD2 in the NAc than susceptible mice. The data presented indicates that viral overexpression of RPRD2 impacts anxiety-like behavior. The data also demonstrates a link between increased RPRD2 levels and decreased S5p levels, indicating a stall in the transcription activity of RNA polymerase II. This RPRD2-mediated regulation of RNA polymerase II phosphorylation may preferentially affect genes involved in microtubule transport, which consequently inhibits the dendritic complexity and function of NAc MSNs. Blunted MSN morphology may be responsible for the increase in anxiety-like behaviors seen in mice. Further analysis of this data may guide future efforts to construct the implications of RPRD2 on Anxiety Disorders and uncover novel molecular pathways to target for treatment efforts.

References

Abcam plc. (n.d.). *Anti-RNA polymerase II antibody (ab264350)*. Abcam.

> https://www.abcam.com/rna-polymerase-ii-antibody-
>
> ab264350.html?productWallTab=ShowAll

Abcam plc. (n.d.). *Anti-RNA polymerase II (phospho S5) antibody (AB240740)*. Abcam.

> https://www.abcam.com/RNA-polymerase-II-phospho-S5-antibody-ab240740.html

Ali, I., Ruiz, D. G., Ni, Z., Johnson, J. R., Zhang, H., Li, P.-C., Conrad, R. J., Guo, X., Min, J.,

> Greenblatt, J., Jacobson, M., Krogan, N. J., & Ott, M. Klkn. (2019). Crosstalk between
>
> RNA Pol II C-Terminal Domain Acetylation and Phosphorylation via RPRD Proteins.
>
> Molecular Cell, 74(6), 1164–1174. https://doi.org/10.1016/j.molcel.2019.04.008

Alliance of Genome Resources. (2021, November). *RPRD2 regulation of nuclear pre-mRNA*

> *domain containing 2*. National Center for Biotechnology Information.
>
> https://www.ncbi.nlm.nih.gov/gtr/genes/23248/

Anxiety & Depression Association of America (Ed.). (2021, September 19). *Facts & Statistics*.

> Anxiety and Depression Association of America, ADAA. https://adaa.org/understanding-
>
> anxiety/facts-statistics

Bagot, R. C., Parise, E. M., Peña, C. J., Zhang, H. X., Maze, I., Chaudhury, D., Persaud, B.,
Cachope,

> R., Bolaños-Guzmán, C. A., Cheer, J. F., Deisseroth, K., Han, M. H., & Nestler, E. J. (2015).
>
> Ventral hippocampal afferents to the nucleus accumbens regulate susceptibility to
>
> depression. *Nature communications*, *6*, 7062. https://doi.org/10.1038/ncomms8062

Baik, JH. Stress and the dopaminergic reward system. *Exp Mol Med* 52, 1879–1890 (2020).

https://doi.org/10.1038/s12276-020-00532-4

Bailey, K. R., & Crawley, J. N. (2009). Anxiety-Related Behaviors in Mice. Nih.gov; CRC

Press/Taylor & Francis. https://www.ncbi.nlm.nih.gov/books/NBK5221/

Bandelow, B., Michaelis, S., & Wedekind, D. (2017). Treatment of anxiety disorders. *Dialogues in*

clinical neuroscience, *19*(2), 93–107.

https://doi.org/10.31887/DCNS.2017.19.2/bbandelow

Bessa, J. M., Morais, M., Marques, F., Pinto, L., Palha, J. A., Almeida, O. F., & Sousa, N. (2013).

Stress-induced anhedonia is associated with hypertrophy of medium spiny neurons of

the nucleus accumbens. *Translational psychiatry*, *3*(6), e266.

https://doi.org/10.1038/tp.2013.39

Binley, K. E., Ng, W. S., Tribble, J. R., Song, B., & Morgan, J. E. (2014, January 28). *Sholl Analysis:*

A quantitative comparison of semi-automated methods. Journal of Neuroscience

Methods.

https://www.sciencedirect.com/science/article/pii/S0165027014000284#:~:text=sholl%

20analysis%20%28%20sholl%2C%201953%20%29%2C%20is%20a,the%20radial%20dista

nce%20from%20the%20soma%20centre.%20?msclkid=2fef7dababaa11ecbdb14a0c6c6

30353

Bio-Rad Laboratories, Inc. (n.d.). *General Protocol for Western Blotting*. Bio-rad.com.

https://www.bio-rad.com/webroot/web/pdf/lsr/literature/Bulletin_5637B.pdf

Daroff, R. B., & Aminoff, M. J. (2014). Nervous System, Neuroembryology of. In *Encyclopedia of*

the Neurological Sciences (second edition) (pp. 350–359). essay, Academic Press.

Dent E. W. (2017). Of microtubules and memory: implications for microtubule dynamics in dendrites and spines. *Molecular biology of the cell*, *28*(1), 1–8. https://doi.org/10.1091/mbc.E15-11-0769

Dobrof, R., & Penrod-Martin. (2012, May 1). *Morphological characterization of medium spiny neuron development in vitro*. Libraries digital conservancy. https://conservancy.umn.edu/handle/11299/151475

Dorrier, C. E., Jones, H. E., Pintarić, L., Siegenthaler, J. A., & Daneman, R. (2022). Emerging roles for CNS fibroblasts in health, injury and disease. *Nature reviews. Neuroscience*, *23*(1), 23–34. https://doi.org/10.1038/s41583-021-00525-w

Duffy, B., Danielle, A., Meyer, C., Moxham-Hall, V., Murkin, G., Rubin, J., Strang, L., & Wessely, S.

(2020, April). *The Accepting, the Suffering and the Resisting: the different reactions to life under lockdown*. Coronavirus in the UK Cluster Analysis. https://www.kcl.ac.uk/policy-institute/assets/Coronavirus-in-the-UK-cluster-analysis.pdf

Duman, E. A., & Canli, T. (2015). Influence of life stress, 5-HTTLPR genotype, and SLC6A4 methylation on gene expression and stress response in healthy Caucasian males. *Biology of mood & anxiety disorders*, *5*, 2. https://doi.org/10.1186/s13587-015-0017-x

Francis, T. C., & Lobo, M. K. (2017). Emerging Role for Nucleus Accumbens Medium Spiny Neuron Subtypes in Depression. *Biological psychiatry*, *81*(8), 645–653. https://doi.org/10.1016/j.biopsych.2016.09.007

File, S. E., & Hyde, J. R. (1978). Can social interaction be used to measure anxiety?. *British journal of pharmacology*, *62*(1), 19–24. https://doi.org/10.1111/j.1476-5381.1978.tb07001.x

Franklin, K., & Paxinos, G. (2019). *Paxinos and Franklin's the Mouse Brain in stereotaxic coordinates* (5th ed.). ELSEVIER ACADEMIC Press.

Genomics from Azenta Life Sciences (Ed.). (n.d.). *RNA Sequencing*. GENEWIZ from Azenta | RNA-Seq. https://www.genewiz.com/en/Public/Services/Next-Generation-Sequencing/RNA-Seq

Golden SA, Covington HE, 3rd, Berton O, Russo SJ. A standardized protocol for repeated social defeat stress in mice. *Nat. Protoc.* 2011;6:1183–1191. doi: 10.1038/nprot.2011.361

Hamilton, P. J., Chen, E. Y., Tolstikov, V., Pena, C. J., Picone, J. A., Shah, P., Panagopoulos, K., Strat,

A. N., Walker, D. M., Lorsch, Z. S., Robinson, H. L., Mervosh, N. L., Kiraly, D. D., Sarangarajan, R., Narain, N. R., Kiebish, M. A., & Nestler, E. J. (2020). Chronic stress and antidepressant treatment alter purine metabolism and beta oxidation within mouse brain and serum. Scientific Reports, 10, 18134. doi: 10.1038/s41598-020-75114-5

Herbison, C., Allen, K., Robinson, M., Newnham, J., & Pennell, C. (2017). The impact of life stress on adult depression and anxiety is dependent on gender and timing of exposure. *Development and Psychopathology, 29*(4), 1443-1454. doi:10.1017/S0954579417000372

Hoffman. (2015). Modeling Neuropsychiatric Disorders in Laboratory Animals. ScienceDirect. https://www.sciencedirect.com/book/9780081000991/modeling-neuropsychiatric-disorders-in-laboratory-animals

Kraeuter, A. K., Guest, P. C., & Sarnyai, Z. (2019). The Elevated Plus Maze Test for Measuring

Anxiety-Like Behavior in Rodents. *Methods in molecular biology (Clifton, N.J.)*, *1916*, 69–

74. https://doi.org/10.1007/978-1-4939-8994-2_4

Kukurba, K. R., & Montgomery, S. B. (2015). RNA Sequencing and Analysis. Cold Spring Harbor

Protocols, 2015(11), pdb.top084970. https://doi.org/10.1101/pdb.top084970

LeGates, T. A., Kvarta, M. D., Tooley, J. R., Francis, T. C., Lobo, M. K., Creed, M. C., & Thompson,

S.

M. (2018). Reward behaviour is regulated by the strength of hippocampus-nucleus

accumbens synapses. *Nature*, *564*(7735), 258–262. https://doi.org/10.1038/s41586-

018-0740-8

Lucassen, P. J., Pruessner, J., Sousa, N., Almeida, O. F., Van Dam, A. M., Rajkowska, G., Swaab,

D.

F., & Czéh, B. (2014). Neuropathology of stress. *Acta neuropathologica*, *127*(1), 109–

135. https://doi.org/10.1007/s00401-013-1223-5

Mahmood, T., & Yang, P. C. (2012). Western blot: technique, theory, and trouble shooting.

North

American journal of medical sciences, *4*(9), 429–434. https://doi.org/10.4103/1947-

2714.100998

Marchisella, F., Coffey, E. T., & Hollos, P. (2016). Microtubule and microtubule associated

protein

anomalies in psychiatric disease. *Cytoskeleton (Hoboken, N.J.)*, *73*(10), 596–611.

https://doi.org/10.1002/cm.21300

Mariotti A. (2015). The effects of chronic stress on health: new insights into the molecular

mechanisms of brain-body communication. *Future science OA*, *1*(3), FSO23.

https://doi.org/10.4155/fso.15.21

Mavridis I. (2015). The role of the nucleus accumbens in psychiatric disorders. *Psychiatrike =*

Psychiatriki, *25*(4), 282–294. https://pubmed.ncbi.nlm.nih.gov/26709994

Meunier, A., & Spassky, N. (2020). Ependyma. In K. Sawamoto (Ed.), *Patterning and Cell Type*

Specification in the Developing CNS and PNS (Second Edition) (pp. 1021–1036). essay,

Comprehensive Developmental Neuroscience.

Ni, Z., Olsen, J. B., Guo, X., Zhong, G., Ruan, E. D., Marcon, E., Young, P., Guo, H., Li, J., Moffat, J.,

Emili, A., & Greenblatt, J. F. (2011). Control of the RNA polymerase II phosphorylation

state in promoter regions by CTD interaction domain-containing proteins RPRD1A and

RPRD1B. Transcription, 2(5), 237–242. https://doi.org/10.4161/trns.2.5.17803

Ni, Z., Xu, C., Guo, X., Hunter, G. O., Kuznetsova, O. V., Tempel, W., Marcon, E., Zhong, G., Guo,

H., Kuo, W.-H. W., Li, J., Young, P., Olsen, J. B., Wan, C., Loppnau, P., El Bakkouri, M.,

Senisterra, G. A., He, H., Huang, H., Sidhu, S., Emili, A., Murphy, S., Mosley, A.,

Arrowsmith, C., Min, J., Greenblatt, J. F. RPRD1A and RPRD1B are human RNA

polymerase II C-terminal domain scaffolds for Ser5 dephosphorylation. *Nat Struct Mol*

Biol 21, 686–695 (2014). https://doi.org/10.1038/nsmb

Nikčević, A. V., & Spada, M. M. (2020). The COVID-19 anxiety syndrome scale: Development and

psychometric properties. Psychiatry Research, 292, 113322.

https://doi.org/10.1016/j.psychres.2020.113322

Pêgo, J. M., Sousa, J. C., Almeida, O. F., & Sousa, N. (2010). Stress and the neuroendocrinology

of anxiety disorders. *Current topics in behavioral neurosciences*, *2*, 97–117.

https://doi.org/10.1007/7854_2009_13

Qi, T., Hu, T., Ge, QQ. *et al.* COVID-19 pandemic related long-term chronic stress on the

prevalence of depression and anxiety in the general population. *BMC Psychiatry* 21, 380

(2021). https://doi.org/10.1186/s12888-021-03385-x

Robinson, G. E., Fernald, R. D., & Clayton, D. F. (2008). Genes and social behavior. *Science (New*

York, N.Y.), *322*(5903), 896–900. https://doi.org/10.1126/science.1159277

Rodgers, R. J., & Dalvi, A. (1997). Anxiety, defence and the elevated plus-maze. *Neuroscience*

and biobehavioral reviews, *21*(6), 801–810. https://doi.org/10.1016/s0149-

7634(96)00058-9

Selçuk, E. B., Demir, A. Ç., Erbay, L. G., Özcan, Ö. Ö., Gürer, H., & Dönmez, Y. E. (2021). Anxiety,

depression and post-traumatic stress disorder symptoms in adolescents during the

COVID-19 outbreak and associated factors. *International journal of clinical practice*,

75(11), e14880. https://doi.org/10.1111/ijcp.14880

Sheffler, Z. M. (2021, May 9). *Physiology, neurotransmitters*. StatPearls [Internet].

https://www.ncbi.nlm.nih.gov/books/NBK539894/

Simon, P., Dupuis, R., & Costentin, J. (1994). Thigmotaxis as an index of anxiety in mice.

Influence of dopaminergic transmissions. *Behavioural brain research*, *61*(1), 59–64.

https://doi.org/10.1016/0166-4328(94)90008-6

Sjöstedt E, Zhong W, Fagerberg L, Karlsson M, Mitsios N, Adori C, Oksvold P, Edfors F,

Limiszewska A, Hikmet F, Huang J, Du Y, Lin L, Dong Z, Yang L, Liu X, Jiang H, Xu X, Wang

J, Yang H, Bolund L, Mardinoglu A, Zhang C, von Feilitzen K, Lindskog C, Pontén F, Luo Y,

Hökfelt T, Uhlén M, Mulder J. (2020, March). Brain tissue expression of RPRD2 -

Summary. The Human Protein Atlas. https://www.proteinatlas.org/ENSG00000163125-

RPRD2/brain

Snt ' step-by-step instructions. ImageJ Wiki. (n.d.).

https://imagej.net/plugins/snt/step-by-step-instructions

Srivastava, R., & Ahn, S. H. (2015). Modifications of RNA polymerase II CTD: Connections to the

histone code and cellular function. *Biotechnology advances*, *33*(6 Pt 1), 856–872.

https://doi.org/10.1016/j.biotechadv.2015.07.008

Stoica, L., Ahmed, S. S., Gao, G., & Sena-Esteves, M. (2013). Gene transfer to the CNS using

recombinant adeno-associated virus. *Current protocols in microbiology*, *Chapter 14*,

Unit14D.5. https://doi.org/10.1002/9780471729259.mc14d05s29

Talevi, D., Socci, V., Carai, M., Carnaghi, G., Faleri, S., Trebbi, E., di Bernardo, A., Capelli, F., &

Pacitti, F. (2020). Mental health outcomes of the CoViD-19 pandemic. *Rivista di

psichiatria*, *55*(3), 137–144. https://doi.org/10.1708/3382.33569

Torales, J., O'Higgins, M., Castaldelli-Maia, J. M., & Ventriglio, A. (2020). The outbreak of

COVID-19 coronavirus and its impact on global mental health. *The International journal

of social psychiatry*, *66*(4), 317–320. https://doi.org/10.1177/0020764020915212

Wendelmuth, M., Willam, M., Todorov, H., Radyushkin, K., Gerber, S., & Schweiger, S. (2020).

Dynamic longitudinal behavior in animals exposed to chronic social defeat stress. *PloS

one*, *15*(7), e0235268. https://doi.org/10.1371/journal.pone.0235268

Vita

Claire was raised in Vienna, VA and matriculated into William & Mary in Williamsburg, VA where she received her Bachelor of Science in Kinesiology & Health Sciences, Public Health Concentration and a minor in Chemistry in 2020. She received her Pre-Medical Graduate Health-Sciences Certificate in 2021 from Virginia Commonwealth University's School of Medicine in Richmond, VA. At present, Claire is attending Virginia Commonwealth University's School of Medicine and expects to graduate with a Master of Science in Anatomy and Neurobiology in 2022.